NNLO Parton Distributions and $\alpha_s(M_Z^2)$ for the LHC

Johannes Blümlein
DESY

in collaboration with Sergey Alekhin, Helmut Böttcher, and Sven-Olaf Moch

[arXiv:1202.2700, Phys. Rev. **D** (2012) and in preparation]

Physics in Collision Strbske Pleso, Slovakia September 2012

Contents

References

- ABKM09: S. Alekhin, JB, S. Klein, S.-O. Moch arXiv:0908.2766
- ABM10: S. Alekhin, JB, S.-O. Moch arXiv:1007.3657
- ABM11: S. Alekhin, JB, S.-O. Moch arXiv:1202.2281
- NNLO benchmark cs at the Terascale: S. Alekhin, JB, P. Jimenez-Delgado, S.-O. Moch, E. Reya, arXiv:1011.6259
- Fixed target data and Higgs Prod. Rates: S. Alekhin, JB, S.-O. Moch arXiv:1101.5261

References below will mostly be used in terms of acronyms, like "MSTW08" etc.

Introduction

- Precision determinations of parton distribution functions (PDFs) and $\alpha_s(M_Z^2)$ are currently being performed at NNLO (α_s^3).
- NLO fits suffer from scale uncertainties being too large.
- The heavy flavor corrections are available in NLO + threshold corrections and the calculation of the NNLO corrections is making progress.
- Sensitive data, capable to constrain the known PDFs better, have to be selected, rather than performing global analyses using data with problematic systematics.
- Current data: DIS World data (including H1+ZEUS combined); Di-muon data (s); Drell-Yan data ($\bar{d} - \bar{u}$); pp-jet data: LHC data will take over very soon; Likewise: $W^{\pm}, Z$ off-resonance Drell-Yan at LHC.
- α_s and HT terms have to be fitted along with the non-pert. parameters of the PDFs.

Introduction

- Heavy flavor treatment: BMSN-interpolation from threshold to asymptotia; observe all relations implied by the RGE Bierenbaum, JB, Klein, 2009.
- Deuteron wave function corrections and Traget Mass corrections are mandatory.
- Characterize the fit publishing the covariance matrices.
- Soft Resummation: heavy flavor threshold; NS Wilson coefficients beyond 3-loop; Effect on the HT-terms.
- We will compare most of the results with those obtained by other fitting groups.
- Predictions are made for main scattering cross sections at Tevatron and the LHC.

The Data

	Experiment	NDP	χ^2(NNLO)	χ^2(NLO)
DIS inclusive	H1&ZEUS	486	537	531
	H1	130	137	132
	BCDMS	605	705	695
	NMC	490	665	661
	SLAC-E-49a	118	63	63
	SLAC-E-49b	299	357	357
	SLAC-E-87	218	210	219
	SLAC-E-89a	148	219	215
	SLAC-E-89b	162	133	132
	SLAC-E-139	17	11	11
	SLAC-E-140	26	28	29
Drell-Yan	FNAL-E-605	119	167	167
	FNAL-E-866	39	52	55
DIS di-muon	NuTeV	89	46	49
	CCFR	89	61	62
Total		3036	3391	3378

Tabelle 2: The value of χ^2 obtained in the NNLO and NLO fits for different data sets.

Deuteron Corrections

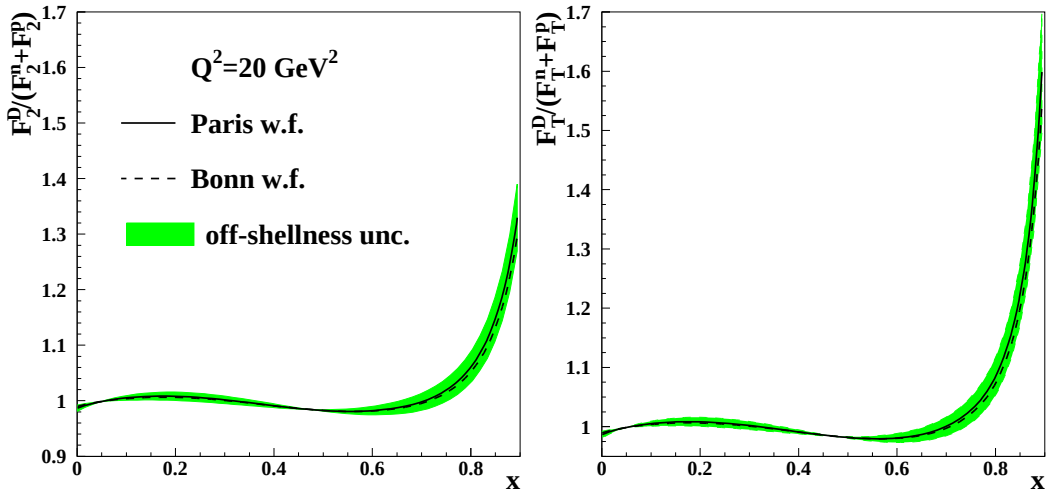

Figure 1: The ratio of the deuterium structure function F_2 (left) and F_T (right) with account of the Fermi-motion and off-shellness effects of [Kulagin 2004] calculated for the Paris potential of (solid) and the Bonn potential (dashes) at the momentum transfer of 20 GeV^2 to the sum of those for free proton and neutron versus x. The shaded area around the solid line gives the uncertainty due to a variation of the off-shell effects by 50%. The calculations are performed at NNLO QCD accuracy using the PDFs and the twist-4 terms obtained by ABKM.

The Fit Parameters

$$
\begin{aligned}
Q_0^2 &= 9\mathrm{GeV}^2 \\
xq_v(x,Q_0^2) &= A_v x^{(a_v+P_v(x))}(1-x)^{b_v} \\
xu_s(x,Q_0^2) &= A_{us} x^{(a_{us}+P_{us}(x))}(1-x)^{b_{us}} \\
\Delta(x,Q_0^2) &= x\bar{d} - x\bar{u} = A_\Delta x^{a_\Delta}(1-x)^{b_\Delta} \\
xs(x,Q_0^2) &= A_s x^{a_s}(1-x)^{b_s} \\
xg(x,Q_0^2) &= A_g x^{(a_g+P_g(x))}(1-x)^{b_g}
\end{aligned}
$$

	a	b	γ_1	γ_2	γ_3	A
u_v	0.712 ± 0.081	3.637 ± 0.138	0.593 ± 0.774	-3.607 ± 0.762	3.718 ± 1.148	
d_v	0.741 ± 0.157	5.123 ± 0.394	1.122 ± 1.232	-2.984 ± 1.077		
u_s	-0.363 ± 0.035	7.861 ± 0.433	4.339 ± 1.790		0.0280 ± 0.0036	0.0808 ± 0.0122
Δ	0.70 ± 0.28	11.75 ± 1.97	-2.57 ± 3.12			0.316 ± 0.385
s	-0.240 ± 0.055	7.98 ± 0.65				0.085 ± 0.017
g	-0.170 ± 0.012	10.71 ± 1.43	4.00 ± 4.21			

Tabelle 1: The parameters of the PDFs in and their 1σ errors obtained in the scheme with $n_f = 3$ flavors.

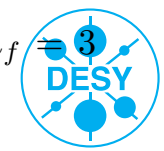

Covariance Matrix

Table 12: The covariance matrix for the PDF parameters, α_s, m_c and m_b.

	a_u	b_u	$\gamma_{1,u}$	$\gamma_{2,u}$	a_d	b_d	A_Δ	b_Δ	A_{us}	a_{us}	b_{us}	a_g	b_g	$\gamma_{1,g}$
a_u	1.0000	0.9692	0.9787	-0.7929	0.7194	0.5279	-0.1460	-0.1007	0.7481	0.6835	-0.4236	-0.2963	0.3391	0.3761
b_u		1.0000	0.9396	-0.7244	0.6792	0.4939	-0.1146	-0.1099	0.7404	0.6840	-0.4146	-0.3138	0.3464	0.3738
$\gamma_{1,u}$			1.0000	-0.8940	0.6506	0.4646	-0.1865	-0.0539	0.6728	0.6093	-0.4799	-0.2755	0.3441	0.3717
$\gamma_{2,u}$				1.0000	-0.4102	-0.2267	0.2357	-0.0182	-0.4075	-0.3495	0.4543	0.1713	-0.3156	-0.3149
a_d					1.0000	0.8827	-0.2155	-0.1964	0.6875	0.6435	-0.3030	-0.3354	0.2635	0.3500
b_d						1.0000	-0.2462	-0.0979	0.5359	0.5099	-0.2957	-0.3443	0.3157	0.3763
A_Δ							1.0000	-0.2068	-0.0689	-0.0698	0.2381	-0.0168	0.0384	0.0453
b_Δ								1.0000	0.1015	0.1279	-0.4146	-0.0852	-0.1185	-0.0892
A_{us}									1.0000	0.9884	-0.4678	-0.4679	0.1961	0.2504
a_{us}										1.0000	-0.4520	-0.5195	0.1982	0.2596
b_{us}											1.0000	0.1436	0.0444	-0.0180
a_g												1.0000	-0.6289	-0.7662
b_g													1.0000	0.9392
$\gamma_{1,g}$														1.0000

Covariance Matrix

Table 13: The covariance matrix for the PDF parameters, α_s, m_c and m_b.

	$\alpha_s(\mu_0)$	$\gamma_{1,\Delta}$	$\gamma_{1,us}$	$\gamma_{1,d}$	$\gamma_{2,d}$	A_s	b_s	a_s	$\gamma_{3,u}$	$m_c(m_c)$	$\gamma_{3,us}$	$m_b(m_b)$	a_Δ
a_u	-0.0435	0.0000	-0.8480	0.6008	0.1535	-0.0034	-0.0437	-0.0355	0.8111	0.0796	-0.4797	0.0044	-0.1718
b_u	-0.1251	0.0316	-0.8375	0.5537	0.1806	0.0008	-0.0345	-0.0276	0.7001	0.0625	-0.4889	-0.0005	-0.1452
$\gamma_{1,u}$	-0.0849	-0.0637	-0.8133	0.5422	0.1667	-0.0324	-0.0671	-0.0638	0.8948	0.0726	-0.4033	0.0075	-0.2028
$\gamma_{2,u}$	0.0920	0.1659	0.5760	-0.3308	-0.2276	0.0799	0.0966	0.1098	-0.9749	-0.0631	0.1728	-0.0142	0.2353
a_d	-0.0321	-0.0137	-0.7618	0.9630	-0.1842	0.0007	-0.0414	-0.0167	0.4878	0.0227	-0.4735	-0.0078	-0.2088
b_d	-0.1666	-0.1167	-0.6060	0.9351	-0.5969	-0.0064	-0.0249	-0.0203	0.3007	-0.0045	-0.3782	-0.0132	-0.2121
A_Δ	0.0206	0.8718	0.1649	-0.2544	0.1916	-0.0232	-0.0212	-0.0294	-0.2398	0.0202	0.0667	0.0034	0.9721
b_Δ	0.0086	-0.6291	-0.1067	-0.1834	-0.1103	0.0594	0.0577	0.0711	0.0052	-0.0063	-0.1768	-0.0083	-0.0662
A_{us}	0.0043	-0.0481	-0.8662	0.5862	0.0768	-0.0341	-0.0659	-0.0493	0.4485	0.1559	-0.8164	-0.0008	-0.0417
a_{us}	-0.0459	-0.0650	-0.8255	0.5493	0.0606	-0.0119	-0.0441	-0.0255	0.3870	0.0940	-0.8628	-0.0055	-0.0375
b_{us}	-0.0382	0.3783	0.7032	-0.3288	0.1278	-0.0734	-0.0445	-0.0807	-0.4262	-0.0100	0.3911	0.0040	0.1782
a_g	0.3785	0.0061	0.3050	-0.3280	0.1338	0.0936	0.0718	0.1165	-0.1744	-0.0137	0.4886	0.0323	-0.0360
b_g	-0.6085	0.1017	-0.0873	0.2827	-0.2104	-0.0543	-0.0114	-0.1223	0.2973	0.1560	-0.1337	0.0141	0.0066
$\gamma_{1,g}$	-0.4642	0.1021	-0.1778	0.3605	-0.1962	-0.0708	-0.0396	-0.1230	0.3132	0.0425	-0.1977	0.0071	0.0201

Covariance Matrix

Table 14: The covariance matrix for the PDF parameters, α_s, m_c and m_b.

	$\alpha_s(\mu_0)$	$\gamma_{1,\Delta}$	$\gamma_{1,us}$	$\gamma_{1,d}$	$\gamma_{2,d}$	A_s	b_s	a_s	$\gamma_{3,u}$	$m_c(m_c)$	$\gamma_{3,us}$	$m_b(m_b)$	a_Δ
$\alpha_s(\mu_0)$	1.0000	0.0176	-0.0394	-0.0798	0.2357	-0.0018	-0.0982	-0.0075	-0.0291	0.1904	0.0676	0.0562	0.0136
$\gamma_{1,\Delta}$		1.0000	0.1183	-0.0802	0.2640	-0.0427	-0.0489	-0.0550	-0.1595	0.0193	0.0985	0.0069	0.7657
$\gamma_{1,us}$			1.0000	-0.6753	-0.0493	-0.0525	0.0158	-0.0445	-0.6039	-0.0656	0.6590	0.0017	0.1487
$\gamma_{1,d}$				1.0000	-0.4041	-0.0213	-0.0513	-0.0366	0.4145	0.0148	-0.3931	-0.0086	-0.2284
$\gamma_{2,d}$					1.0000	0.0308	-0.0016	0.0326	0.1801	0.0276	-0.0510	0.0111	0.1212
A_s						1.0000	0.8570	0.9749	-0.0664	-0.0206	-0.4355	0.0017	-0.0139
b_s							1.0000	0.8730	-0.0894	-0.0706	-0.3708	0.0005	-0.0127
a_s								1.0000	-0.0967	-0.1234	-0.4403	-0.0050	-0.0172
$\gamma_{3,u}$									1.0000	0.0674	-0.2082	0.0153	-0.2378
$m_c(m_c)$										1.0000	-0.0010	0.0505	0.0141
$\gamma_{3,us}$											1.0000	0.0083	0.0276
$m_b(m_b)$												1.0000	0.0006
a_Δ													1.0000

HERA NC Data

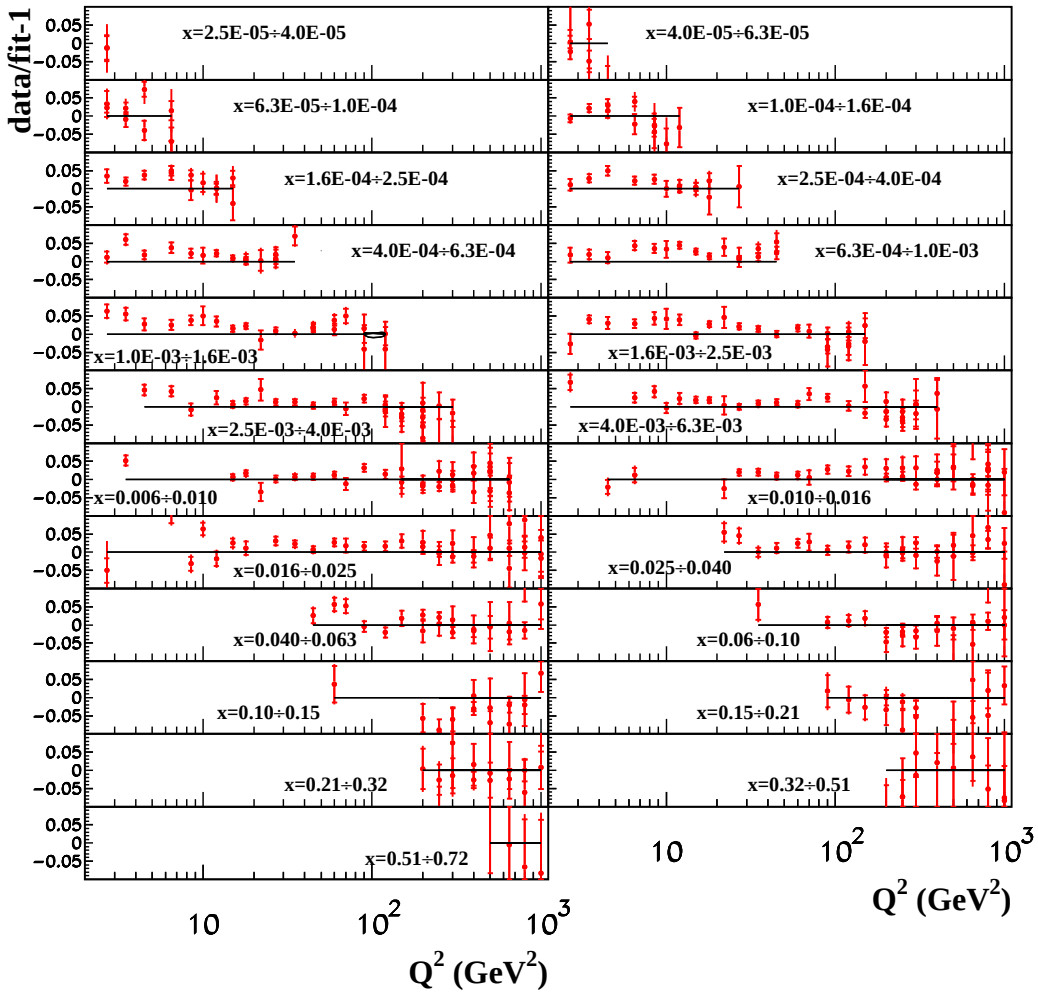

Figure 2: The pulls versus momentum transfer Q^2 for the HERA neutral-current inclusive DIS cross section data of [H1ZEUS09] binned in x with respect to our NNLO fit. The data points with different inelasticity y still may overlap in the plot. The inner bars show statistical errors in data and the outer bars the statistical and systematic errors combined in quadrature.

DESY

HERA CC Data

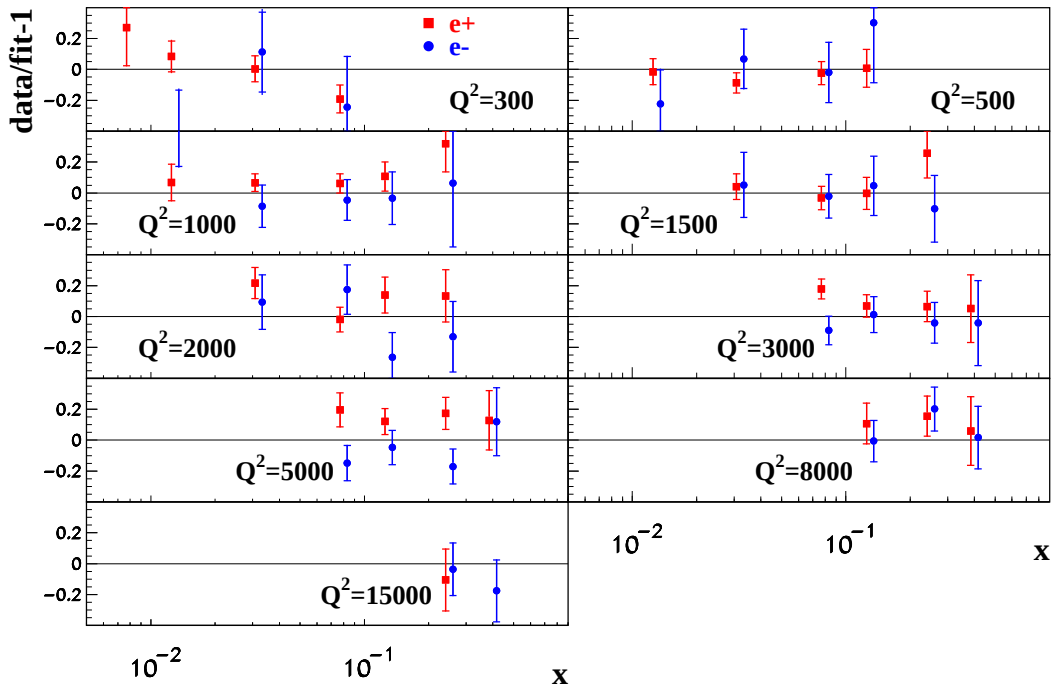

Figure 3: The same as Fig. 2 for the pulls of the HERA charged-current inclusive DIS cross section data of [H1ZEUS09] binned in the momentum transfer Q^2 in units of GeV^2 versus x (squares: positron beam; circles: electron beam).

HERA Low Q^2 Data

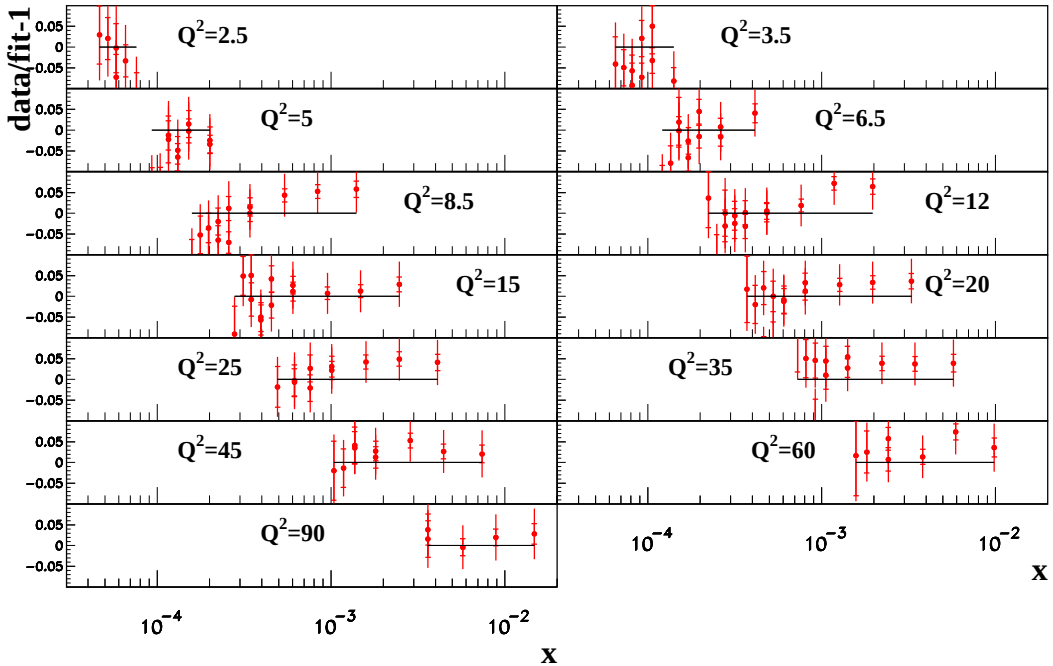

Figure 4: The same as Fig. 2 for the pulls of the H1 neutral-current inclusive DIS cross section data of [H12010] binned in the momentum transfer Q^2 in units of GeV^2 versus x.

BCDMS Data

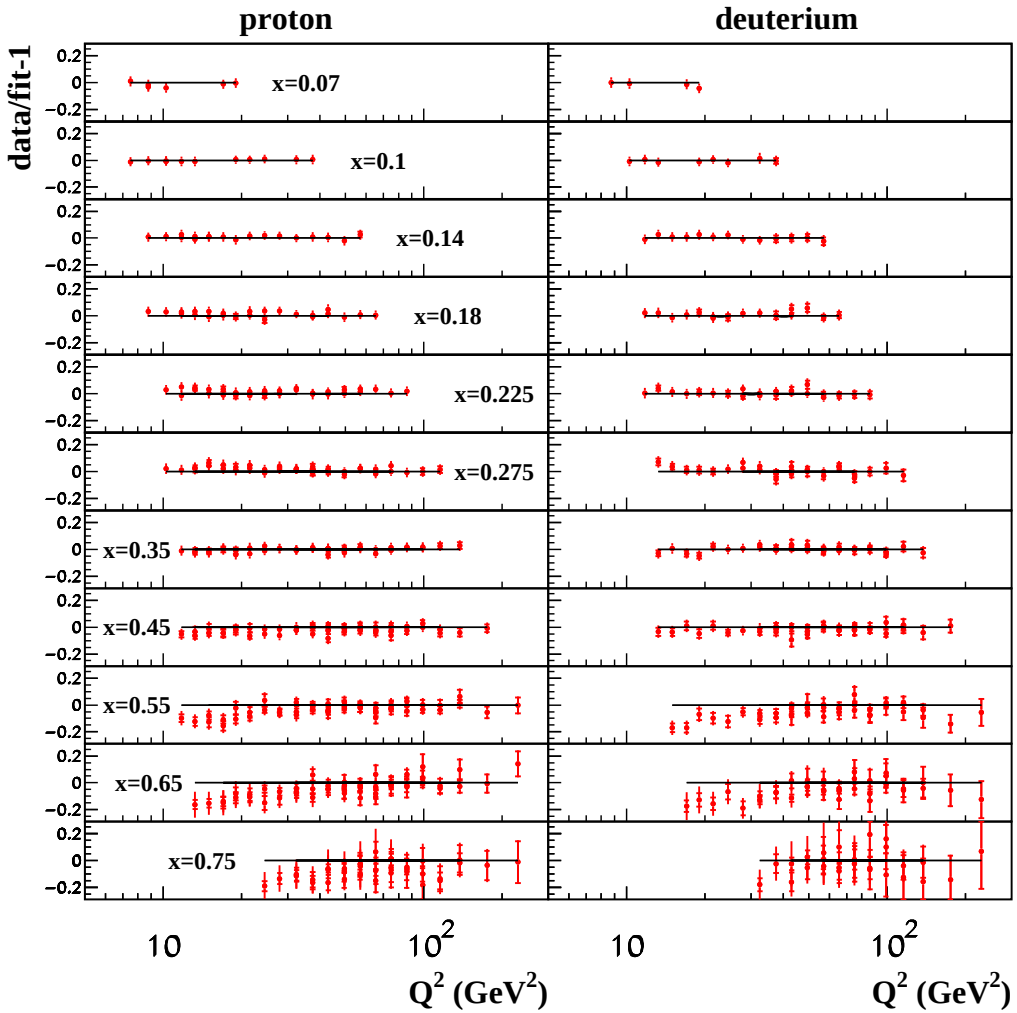

Figure 5: The same as Fig. 2 for the pulls of the BCDMS inclusive DIS cross section data for the proton target (left) and for the deuterium target (right).

NMC Data

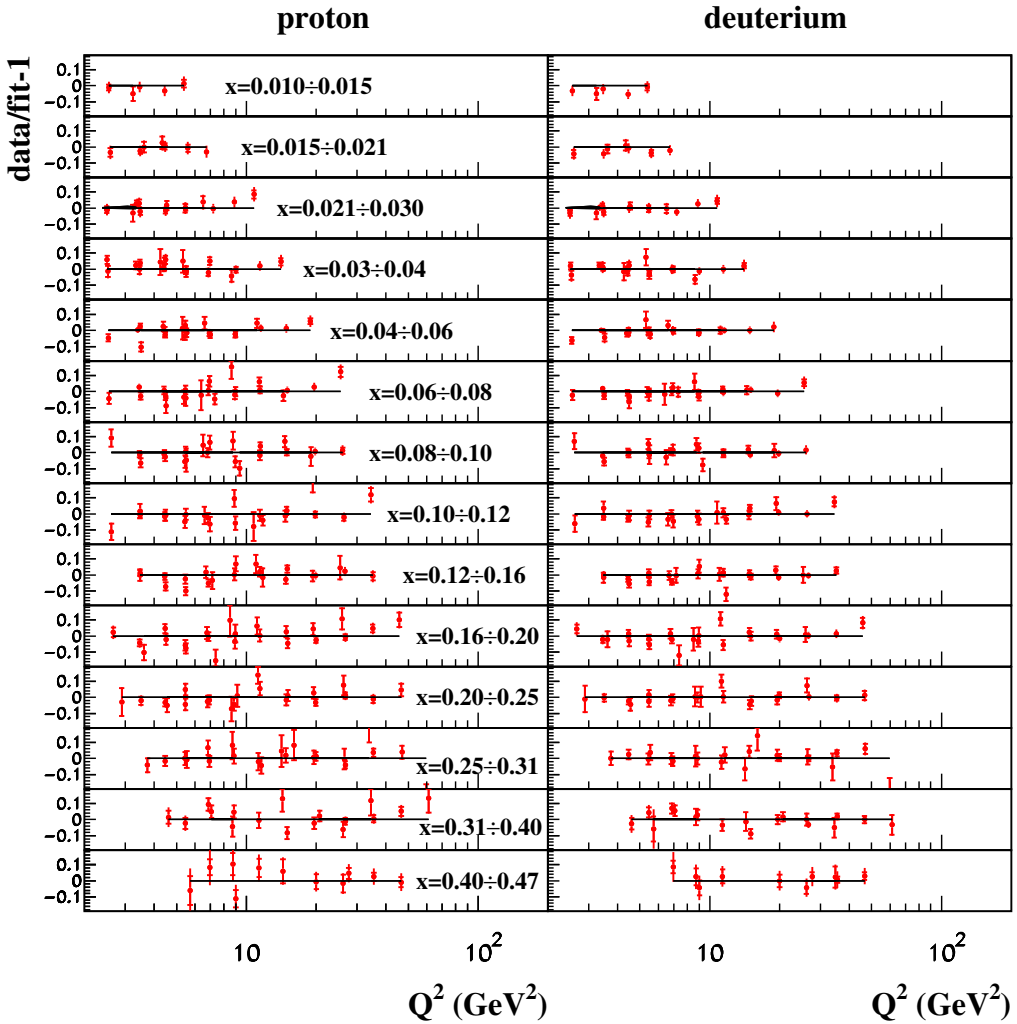

Figure 6: The same as Fig. 2 for the pulls of the NMC inclusive DIS cross section data for the proton target (left) and for the deuterium target (right).

SLAC Data

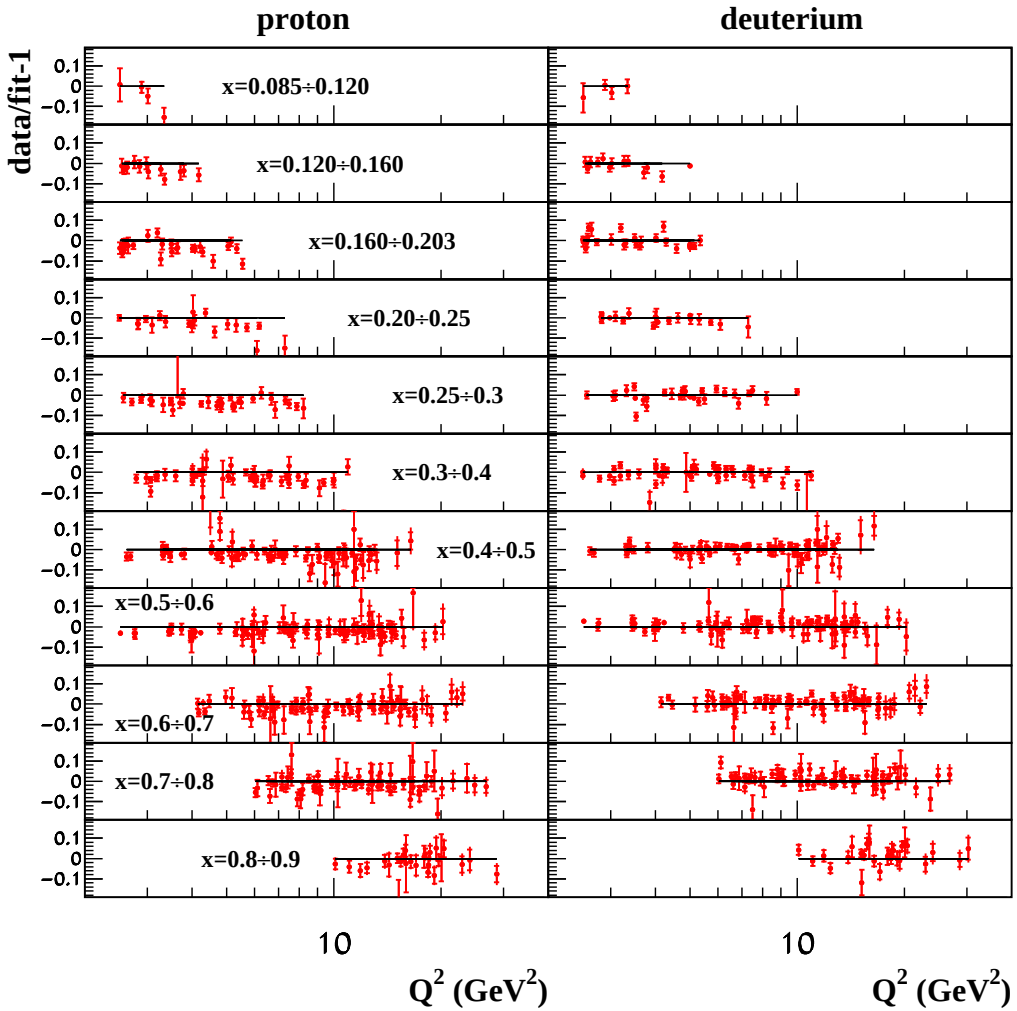

Figure 7: The same as Fig. 2 for the pulls of the SLAC inclusive DIS cross section data for the proton target (left) and for the deuterium target (right).

Di-Muon Data

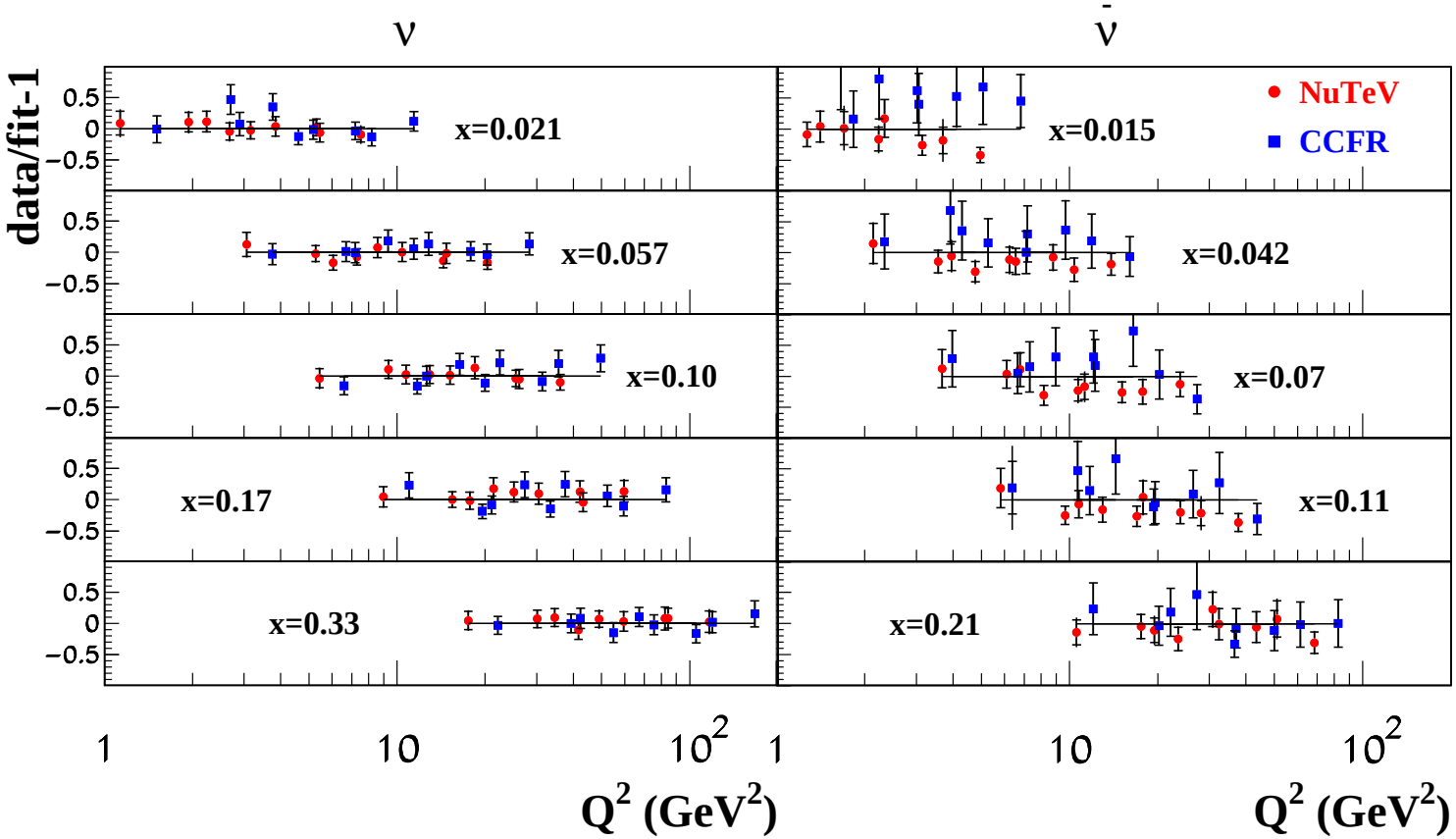

Figure 8: The same as Fig. 2 for the pulls of neutrino (left) and anti-neutrino (right) induced di-muon production cross section data (circles: NuTeV experiment, squares: CCFR experiment).

The Drell-Yan Data

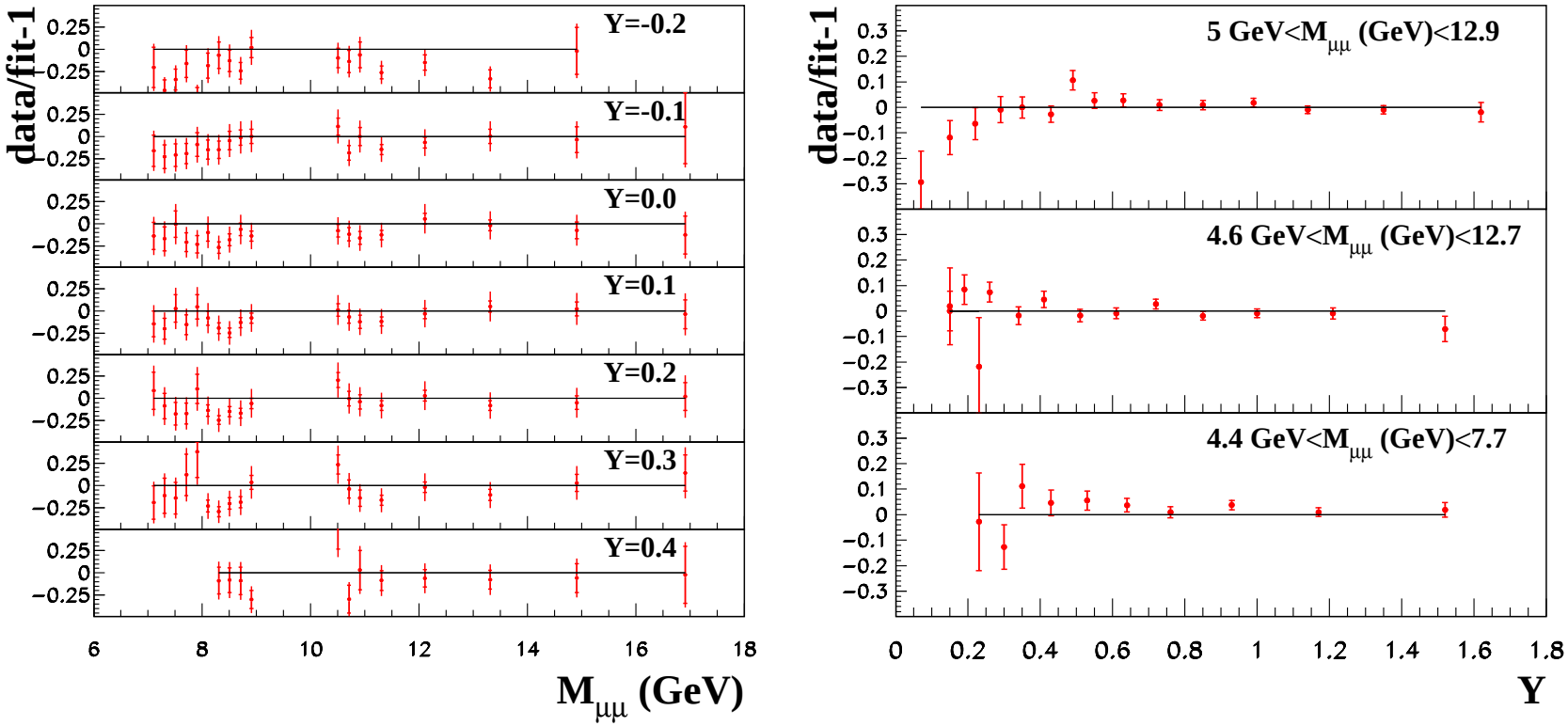

Figure 9: The same as Fig. 2 for the pulls of the DY process cross section data [Moreno90] binned in the muon pair rapidity Y versus the invariant mass $M_{\mu\mu}$ of the muon pair (left) and the ones of [Towell01] binned in $M_{\mu\mu}$ versus Y (right).

ABM11: Fit Results

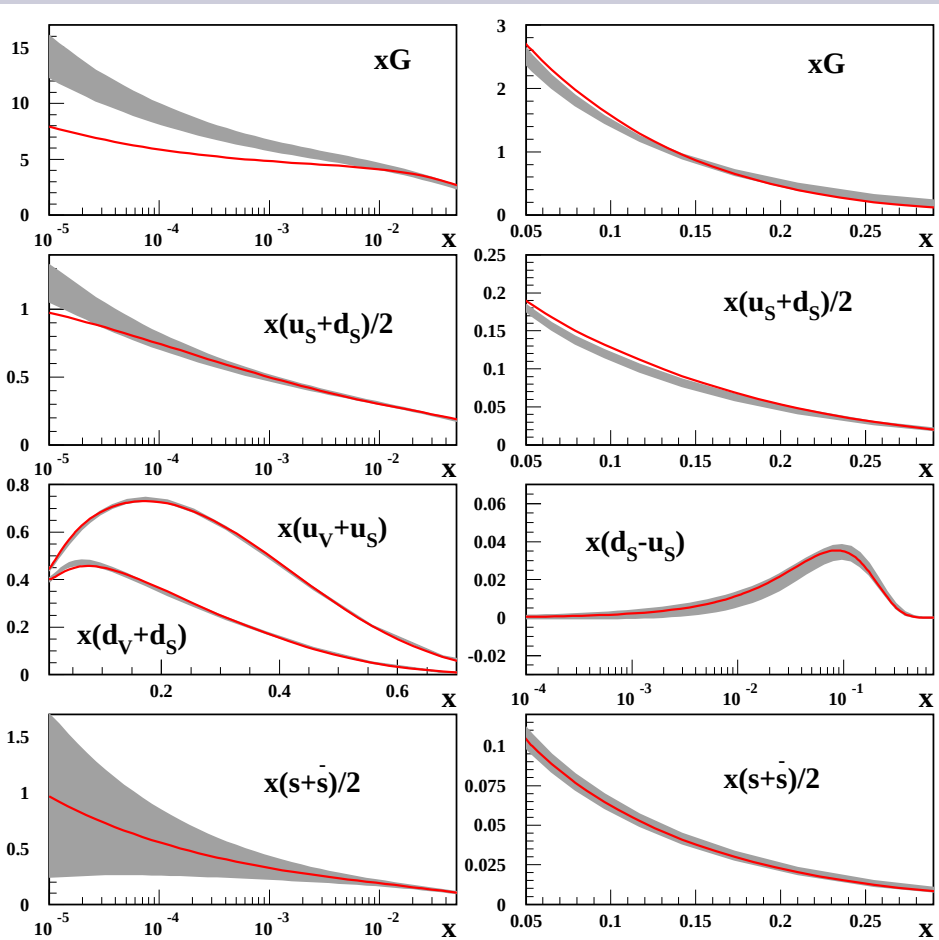

Figure 13: The 1σ band for the 4-flavor NNLO ABKM09 PDFs at the scale of $\mu = 2$ GeV versus x (shaded area) compared with the central values for ones of this analysis (solid lines).

ABM11: Fit Results

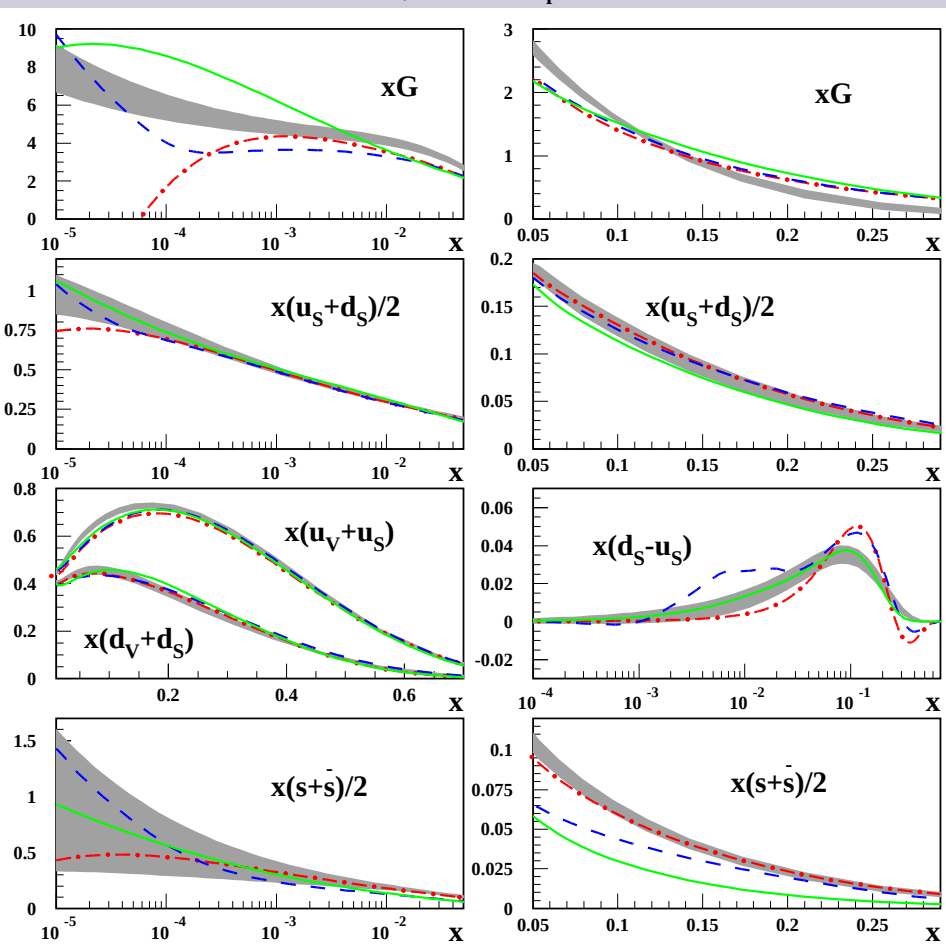

Figure 14: The 1σ band for the 4-flavor NNLO ABM11 PDFs at the scale of $\mu = 2$ GeV versus x obtained in this analysis (shaded area) compared with the ones obtained by other groups (solid lines: JR09, dashed dots: MSTW08, dashes: NN21.

$R(x, Q^2)$

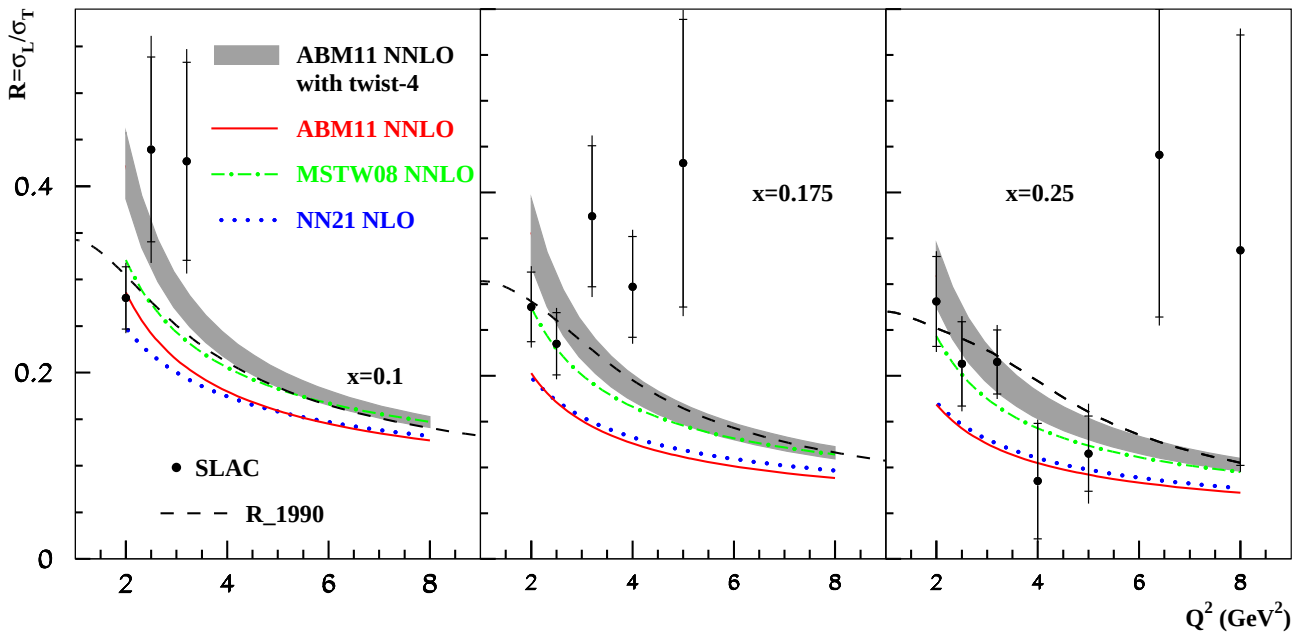

Figure 12: The shaded area gives 1σ band of the NNLO predictions for the ratio $R = \sigma_L/\sigma_T$ based on the ABM11 PDFs and the twist-4 terms obtained from our fit at different values of x versus the momentum transfer Q^2. The central values of the NNLO predictions for R based on the MSTW PDFs (dashed dots), the NNLO predictions based on the ABM11 PDFs (solid line), and the NLO predictions based on the NN21 PDFs (dots), all taken in the 3-flavor scheme and without twist-4 terms, are given for comparison. The data points show values of R extracted from the SLAC proton and deuterium data with the empirical parameterization of those data R_{1990} superimposed (dashes).

$F_L(x, Q^2)$

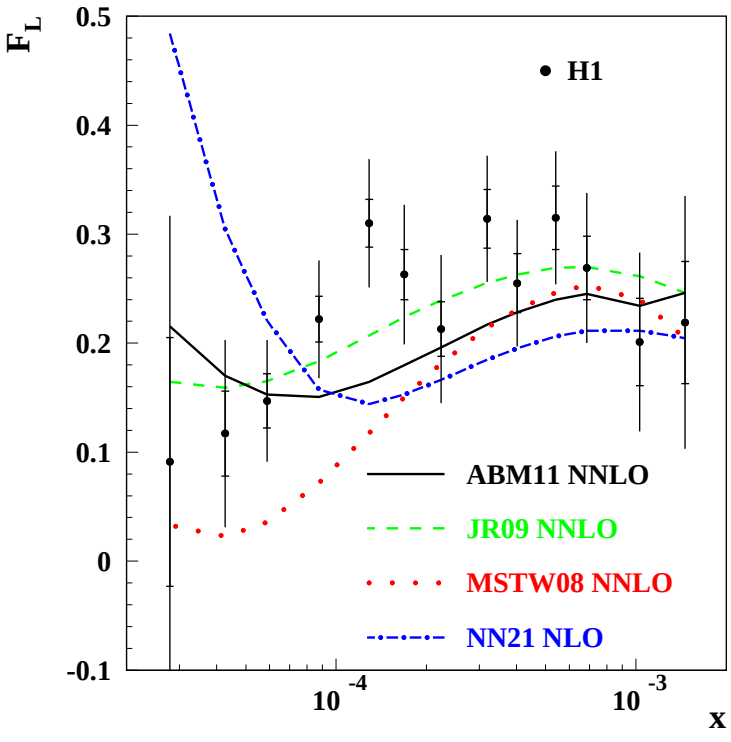

Figure 15: The data on F_L versus x obtained by the H1 collaboration [H12010] confronted with the 3-flavor scheme NNLO predictions based on the different PDFs (solid line: this analysis, dashes: JR09, dots: MSTW08. The NLO predictions based on the 3-flavor NN21 PDFs are given for comparison (dashed dots). The value of Q^2 for the data points and the curves in the plot rises with x in the range of $1.5 \div 45$ GeV^2.

2nd Moment for Valence PDFs

$$xV(x,Q^2) = x[u(x,Q^2) + \bar{u}(x,Q^2) - u(d,Q^2) + \bar{d}(x,Q^2)]$$

	$\langle xu_v(x)\rangle$	$\langle xd_v(x)\rangle$	$\langle x[u_v - d_v](x)\rangle$	$\langle xV(x)\rangle$
ABM11	0.2971 ± 0.0039	0.1174 ± 0.0050	0.1797 ± 0.0042	0.1655 ± 0.0039
ABKM09	0.2981 ± 0.0025	0.1191 ± 0.0023	0.1790 ± 0.0023	0.1647 ± 0.0022
HERAPDF1.5	$0.2938\ ^{+\ 0.0031}_{-\ 0.0052}$	$0.1264\ ^{+\ 0.0054}_{-\ 0.0059}$	$0.1674\ ^{+\ 0.0043}_{-\ 0.0052}$	$0.1706\ ^{+\ 0.0071}_{-\ 0.0103}$
JR09	0.2897 ± 0.0035	0.1253 ± 0.0052	0.1645 ± 0.0063	0.1513 ± 0.0118
MSTW08	$0.2816\ ^{+\ 0.0051}_{-\ 0.0042}$	$0.1171\ ^{+\ 0.0027}_{-\ 0.0028}$	$0.1645\ ^{+\ 0.0046}_{-\ 0.0034}$	$0.1533\ ^{+\ 0.0041}_{-\ 0.0033}$
NN21	0.2913 ± 0.0038	0.1218 ± 0.0042	0.1695 ± 0.0040	0.1539 ± 0.0030
BBG	0.2986 ± 0.0029	0.1239 ± 0.0026	0.1747 ± 0.0039	
BBG [N^{3}LO]	0.3006 ± 0.0031	0.1252 ± 0.0027	0.1754 ± 0.0041	

Table 11: Comparison of the second moment of the valence quark distributions at NNLO and N^{3}LO obtained in different analyses at $Q^2 = 4$ GeV^2.

Comparison with Lattice Results

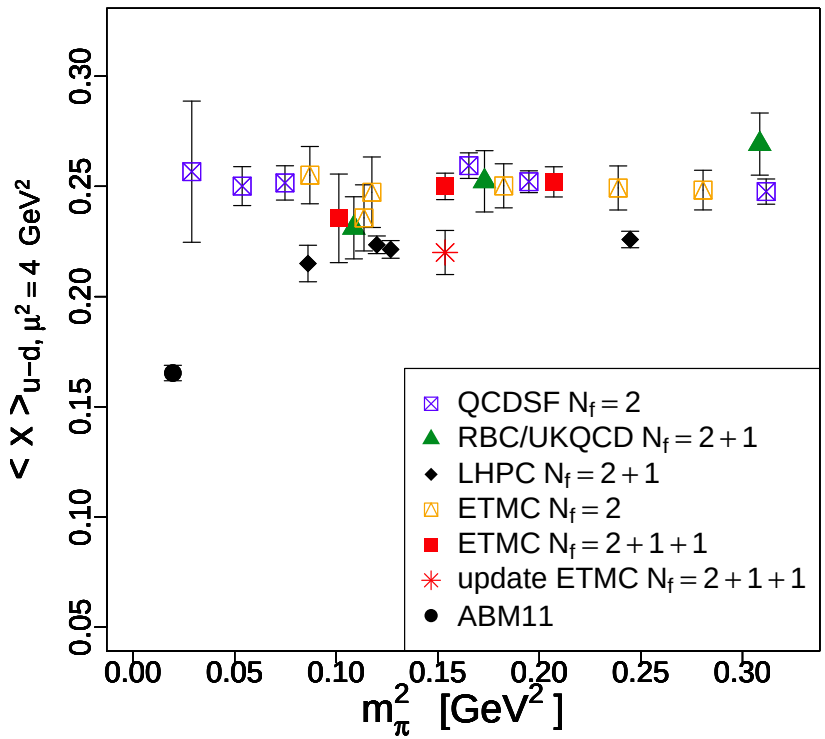

Figure 24: Comparison of lattice computations for the second moment of the non-singlet distribution as a function of the pion mass m_π with the result of ABM11 along with the uncertainties of the respective measurement.

Higher Twist Contributions

ABM11:

$$F_i(x,Q^2) = F_i^{TMC,\tau=2}(x,Q^2) + \frac{H_i^4(x)}{Q^2} + \frac{H_i^6(x)}{Q^4} + \ldots$$

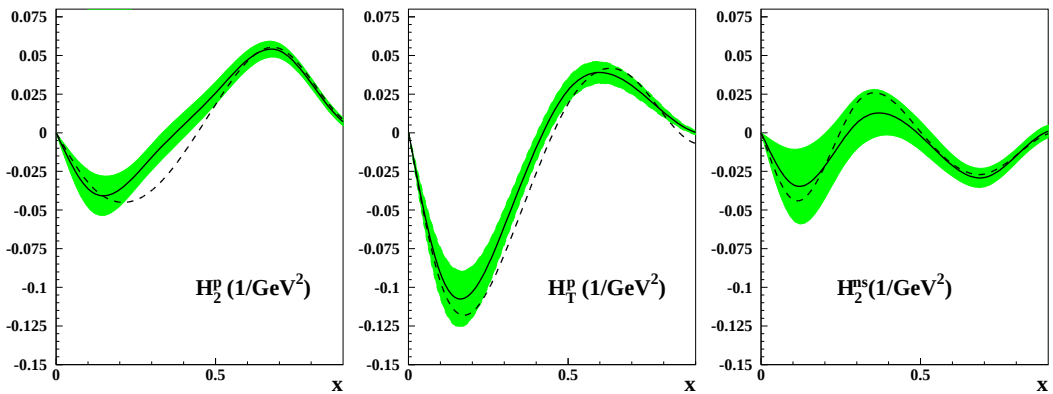

Figure 10: The central values (solid line) and the 1σ bands (shaded area) for the coefficients of the twist-4 terms ofin the inclusive DIS structure functions obtained from our NNLO fit (left panel: F_2 of the proton, central panel: F_T of the proton, right panel: non-singlet F_2). The central values of the twist-4 coefficients obtained from our NLO fit are shown for comparison (dashes).

Higher Twist Contributions

ABM11 :

To completely remove the HT-terms the cut $W^2 > 12.5$ GeV^2, $Q^2 > 10$ GeV^2 is necessary!

	$H_2^{\rm p}(x)/{\rm GeV}^2$	$H_2^{\rm ns}(x)/{\rm GeV}^2$	$H_T^{\rm p}(x)/{\rm GeV}^2$
$x = 0.1$	-0.036 $\pm$ 0.012	-0.034 $\pm$ 0.023	-0.091 $\pm$ 0.017
$x = 0.3$	-0.016 $\pm$ 0.008	0.006 $\pm$ 0.017	-0.061 $\pm$ 0.012
$x = 0.5$	0.026 $\pm$ 0.007	-0.0020 $\pm$ 0.0094	0.0276 $\pm$ 0.0081
$x = 0.7$	0.053 $\pm$ 0.005	-0.029 $\pm$ 0.006	0.031 $\pm$ 0.006
$x = 0.9$	0.0071 $\pm$ 0.0026	0.0009 $\pm$ 0.0041	0.0002 $\pm$ 0.0015

Tabelle 3: The parameters of the twist-4 contribution to the DIS structure functions in for the fit to NNLO accuracy in QCD.

Higher Twist Terms in the Valence Region

J.B. and H. Böttcher, 2012 (BB)
NS-tails at NNLO :

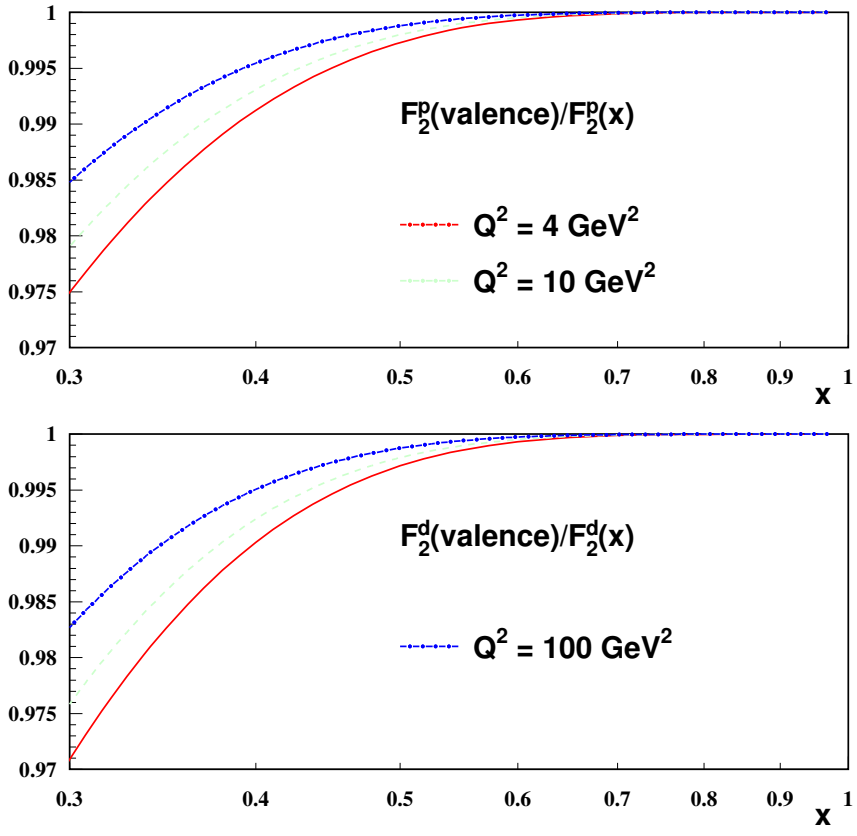

Using ABKM09 we corrected for non NS-tails in $F_2(x, Q^2)$.

$F_2(x, Q^2)$ in the region of larger x

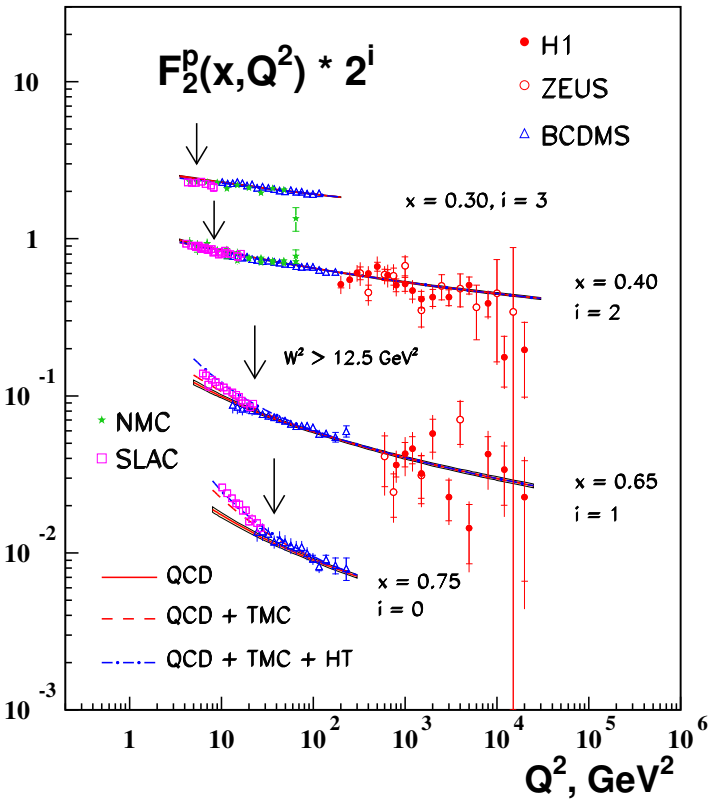

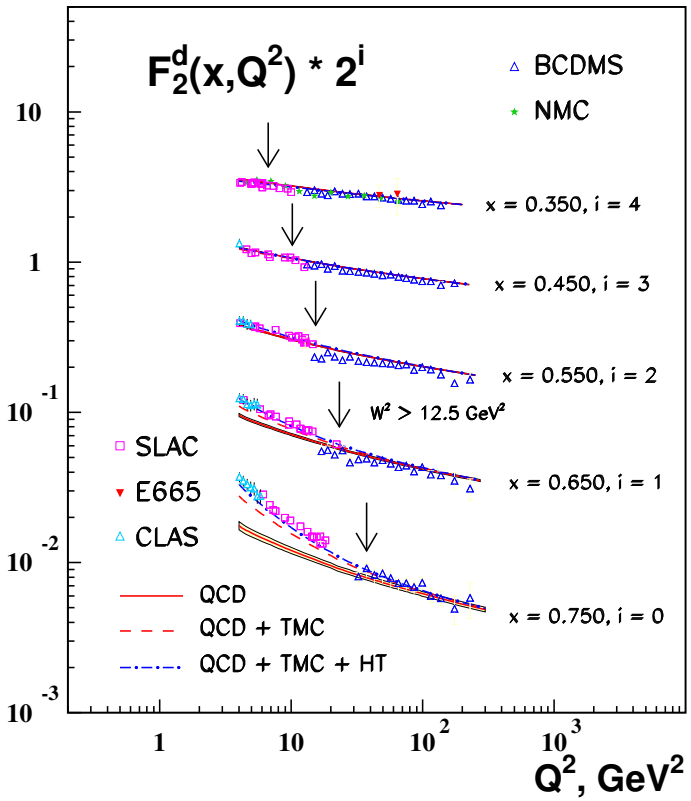

Valence region: HT-terms are removed by the cut
$W^2 > 12.5$ GeV^2, $Q^2 > 4$ GeV^2.

Extracting the Higher Twist Contributions to $F_2(x, Q^2)$

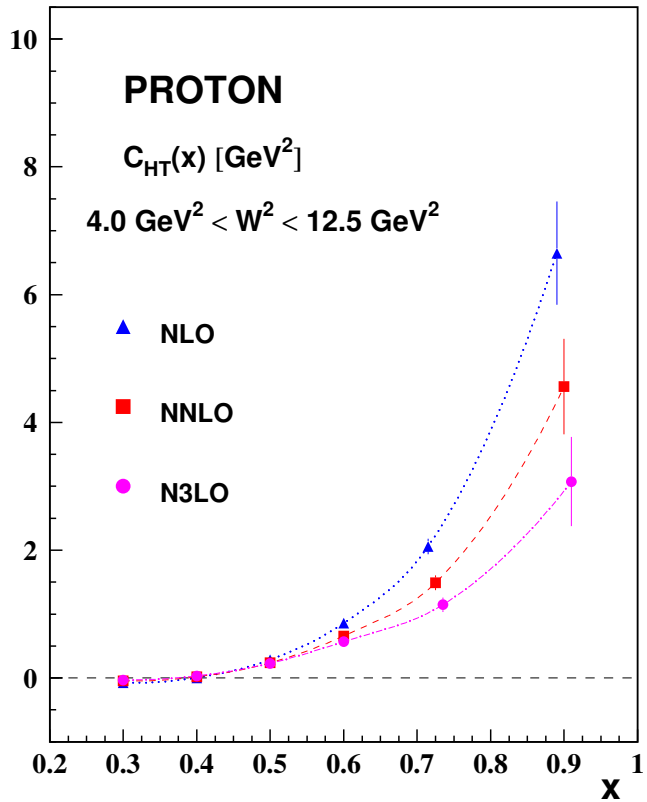

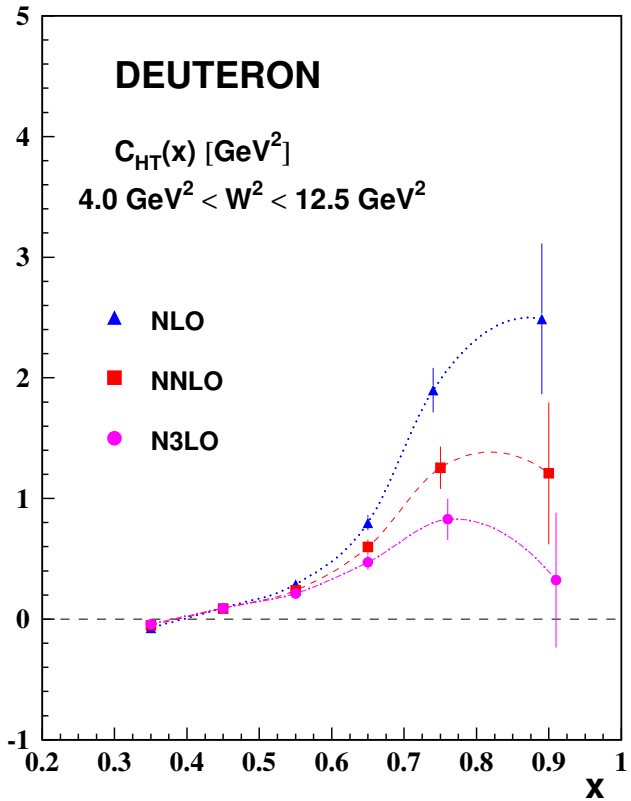

$$F_2(x, Q^2) = F_2^{\tau=2}(x, Q^2)\left[1 + \frac{C(\langle Q^2 \rangle, x)}{Q^2}\right]$$

$\alpha_s(M_Z^2)$

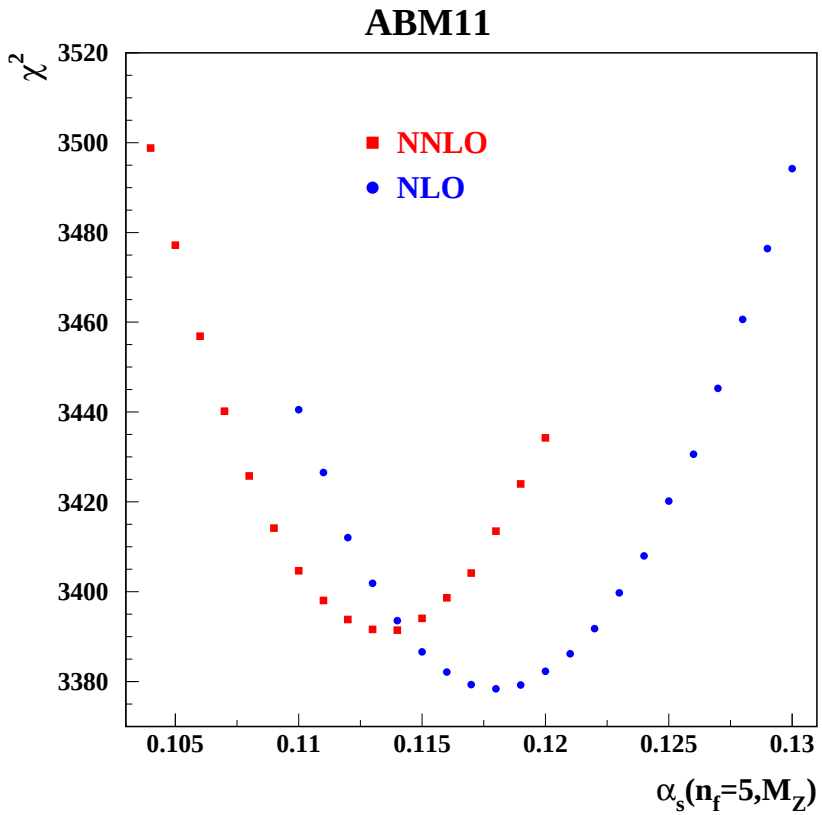

Figure 17: The χ^2-profile as a function of $\alpha_s(M_Z)$ in the present analysis. At NLO (circles) and NNLO (squares).

$\alpha_s(M_Z^2)$

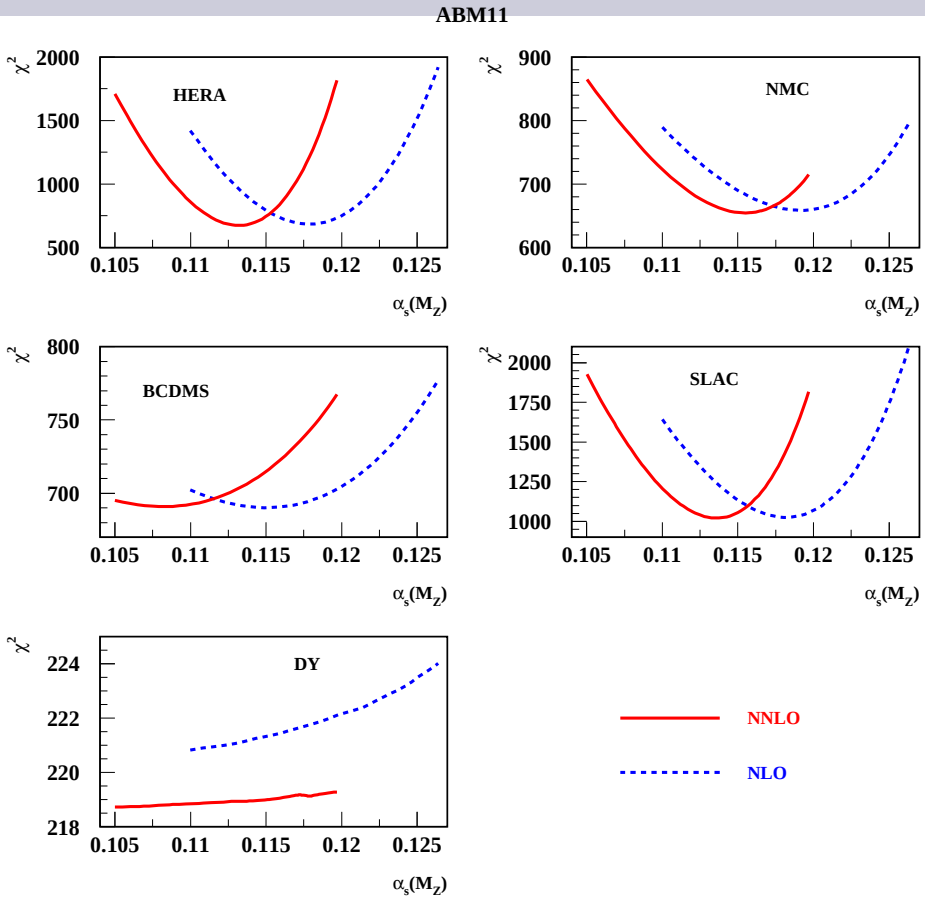

Figure 19: The χ^2-profile versus the value of $\alpha_s(M_Z)$ for the data sets used, all calculated with the PDF and HT parameters fixed at the values obtained from the fits with $\alpha_s(M_Z)$ released (solid lines: NNLO fit, dashes: NLO one).

$\alpha_s(M_Z^2)$

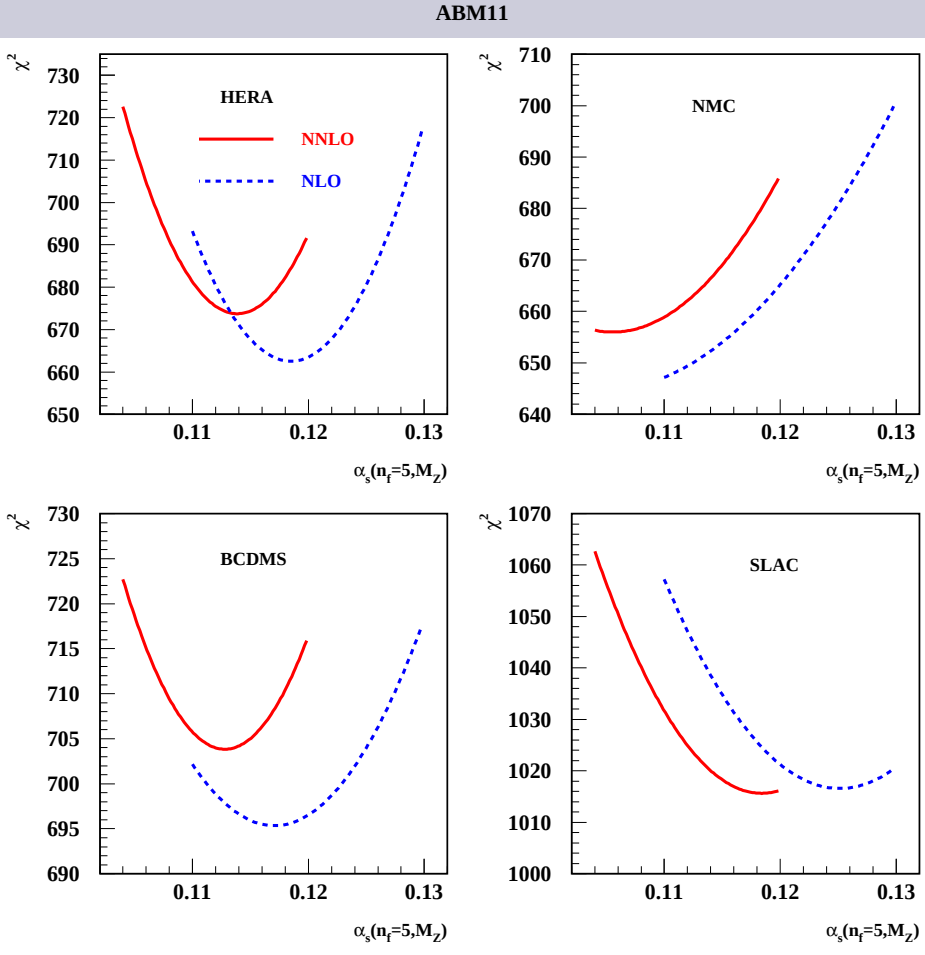

Figure 18: The χ^2-profile versus the value of $\alpha_s(M_Z)$ for the data sets used all obtained in variants of the present analysis with the value of α_s fixed and all other parameters fitted (solid lines: NNLO fit, dashes: NLO fit).

$\alpha_s(M_Z^2)$: ABM11

Experiment	$\alpha_s(M_Z)$		
	NLO_{exp}	NLO	NNLO
BCDMS	0.1111 ± 0.0018	0.1150 ± 0.0012	0.1084 ± 0.0013
NMC	$0.117 \ {}^{+\ 0.011}_{-\ 0.016}$	0.1182 ± 0.0007	0.1152 ± 0.0007
SLAC		0.1173 ± 0.0003	0.1128 ± 0.0003
HERA comb.		0.1174 ± 0.0003	0.1126 ± 0.0002
DY		$0.108 \ \pm 0.010$	$0.101 \ \pm 0.025$
ABM11		0.1180 ± 0.0012	0.1134 ± 0.0011

Tabelle 4: Comparison of the values of $\alpha_s(M_Z)$ obtained by BCDMS and NMC at NLO with the individual results of the fit in the present analysis at NLO and NNLO for the HERA data the NMC data the BCDMS data the SLAC data and the DY data.

$\alpha_s(M_Z^2)$: ABM11 + Tevatron jets

Experiment	$\alpha_s(M_Z)$		
	NLO_{exp}	NLO	NNLO*
D0 1 jet	$0.1161\ ^{+\ 0.0041}_{-\ 0.0048}$	0.1190 ± 0.0011	0.1149 ± 0.0012
D0 2 jet		0.1174 ± 0.0009	0.1145 ± 0.0009
CDF 1 jet (cone)		0.1181 ± 0.0009	0.1134 ± 0.0009
CDF 1 jet ($k_\perp$)		0.1181 ± 0.0010	0.1143 ± 0.0009
ABM11		0.1180 ± 0.0012	0.1134 ± 0.0011

Tabelle 5: Comparison of the values of $\alpha_s(M_Z)$ obtained by D0 with the ones based on including individual data sets of Tevatron jet data into the analysis at NLO. The NNLO* fit refers to the NNLO analysis of the DIS and DY data together with the NLO and soft gluon resummation corrections (next-to-leading logarithmic accuracy) for the 1 jet inclusive data.

$\alpha_s(M_Z^2)$: BBG/BB

Experiment	$\alpha_s(M_Z)$			
	NLO_{exp}	NLO	NNLO	$\mathrm{N^3LO^*}$
BCDMS	0.1111 ± 0.0018	0.1138 ± 0.0007	0.1126 ± 0.0007	0.1128 ± 0.0006
NMC	$0.117 \ {}^{+\ 0.011}_{-\ 0.016}$	0.1166 ± 0.0039	0.1153 ± 0.0039	0.1153 ± 0.0035
SLAC		0.1147 ± 0.0029	0.1158 ± 0.0033	0.1152 ± 0.0027
BBG		0.1148 ± 0.0019	0.1134 ± 0.0020	0.1141 ± 0.0021
BB		0.1147 ± 0.0021	0.1132 ± 0.0022	0.1137 ± 0.0022

Tabelle 6: Comparison of the values of $\alpha_s(M_Z)$ obtained by BCDMS and NMC at NLO with the results of the flavor non-singlet fits BBG and BB of the DIS flavor non-singlet world data, at NLO, NNLO, and $\mathrm{N^3LO^*}$ with the response of the individual data sets, combined for the experiments BCDMS NMC SLAC.

$\alpha_s(M_Z^2)$: NNPDF

Experiment	$\alpha_s(M_Z)$		
	NLO_{exp}	NLO	NNLO
BCDMS	0.1111 ± 0.0018	0.1204 ± 0.0015	0.1158 ± 0.0015
NMC_p		0.1192 ± 0.0018	0.1150 ± 0.0020
NMC_{pd}	$0.117 \ {}^{+\ 0.011}_{-\ 0.016}$		0.1146 ± 0.0107
SLAC		> 0.124	> 0.124
HERA I		0.1223 ± 0.0018	0.1199 ± 0.0019
ZEUS H2		0.1170 ± 0.0027	0.1231 ± 0.0030
ZEUS F2C		0.1144 ± 0.0060	
NuTeV		0.1252 ± 0.0068	0.1177 ± 0.0039
E605		0.1168 ± 0.0100	
E866		0.1135 ± 0.0029	
CDF Wasy		0.1181 ± 0.0060	
CDF Zrap		0.1150 ± 0.0034	0.1205 ± 0.0081
D0 Zrap		0.1227 ± 0.0067	
CDF R2KT		0.1228 ± 0.0021	0.1225 ± 0.0021
D0 R2CON	$0.1161 \ {}^{+\ 0.0041}_{-\ 0.0048}$	0.1141 ± 0.0031	0.1111 ± 0.0029
NN21		0.1191 ± 0.0006	0.1173 ± 0.0007

Tabelle 7: Comparison of the values of $\alpha_s(M_Z)$ obtained by BCDMS, NMC, and D0 at NLO with the results of NN21 for the fits to DIS and other hard scattering data at NLO and NNLO and the corresponding response of the different data sets analysed.

$\alpha_s(M_Z^2)$: MSTW08/09

Experiment	$\alpha_s(M_Z)$		
	NLO$_{exp}$	NLO	NNLO
BCDMS $\mu p, F_2$	0.1111 ± 0.0018	–	0.1085 ± 0.0095
BCDMS $\mu d, F_2$		0.1135 ± 0.0155	0.1117 ± 0.0093
NMC $\mu p, F_2$	$0.117 \; {}^{+\,0.011}_{-\,0.016}$	0.1275 ± 0.0105	0.1217 ± 0.0077
NMC $\mu d, F_2$		0.1265 ± 0.0115	0.1215 ± 0.0070
NMC $\mu n/\mu p$		0.1280	0.1160
E665 $\mu p, F_2$		0.1203	–
E665 $\mu d, F_2$		–	–
SLAC ep, F_2		0.1180 ± 0.0060	0.1140 ± 0.0060
SLAC ed, F_2		0.1270 ± 0.0090	0.1220 ± 0.0060
NMC,BCDMS,SLAC, F_L		0.1285 ± 0.0115	0.1200 ± 0.0060
E886/NuSea pp, DY %citeWebb:2003bj		–	0.1132 ± 0.0088
E886/NuSea pd/pp, DY		0.1173 ± 0.107	0.1140 ± 0.0110
NuTeV $\nu N, F_2$		0.1207 ± 0.0067	0.1170 ± 0.0060
CHORUS $\nu N, F_2$		0.1230 ± 0.0110	0.1150 ± 0.0090
NuTeV $\nu N, xF_3$		0.1270 ± 0.0090	0.1225 ± 0.0075
CHORUS $\nu N, xF_3$		0.1215 ± 0.0105	0.1185 ± 0.0075
CCFR		0.1190	–
NuTeV $\nu N \to \mu\mu X$		0.1150 ± 0.0170	–
H1 ep 97-00, $\sigma_r^{\rm NC}$		0.1250 ± 0.0070	0.1205 ± 0.0055
ZEUS ep 95-00, $\sigma_r^{\rm NC}$		0.1235 ± 0.0065	0.1210 ± 0.0060
H1 ep 99-00, $\sigma_r^{\rm CC}$		0.1285 ± 0.0225	0.1270 ± 0.0200
ZEUS ep 99-00, $\sigma_r^{\rm CC}$		0.1125 ± 0.0195	0.1165 ± 0.0095
H1/ZEUS ep, $F_2^{\rm charm}$		–	0.1165 ± 0.0095
H1 ep 99-00 incl. jets	$0.1168 \; {}^{+\,0.0049}_{-\,0.0034}$	0.1127 ± 0.0093	
ZEUS ep 96-00 incl. jets	$0.1208 \; {}^{+\,0.0048}_{-\,0.0040}$	0.1175 ± 0.0055	
D0 II $p\bar{p}$ incl. jets	$0.1161 \; {}^{+\,0.0041}_{-\,0.0048}$	0.1185 ± 0.0055	0.1133 ± 0.0063
CDF II $p\bar{p}$ incl. jets		0.1205 ± 0.0045	0.1165 ± 0.0025
D0 II $W \to l\nu$ asym.		–	–
CDF II $W \to l\nu$ asym.		–	–
D0 II Z rap.		0.1125 ± 0.0100	0.1136 ± 0.0084
CDF II Z rap.		0.1160 ± 0.0070	0.1157 ± 0.0067
MSTW		$0.1202 \; {}^{+\,0.0012}_{-\,0.0015}$	0.1171 ± 0.0014

Table 8: Comparison of the values of $\alpha_s(M_Z)$ obtained by BCDMS, NMC, HERA-jet and D0 at NLO with the results of the MSTW fits to DIS and other hard scattering data at NLO and NNLO and the corresponding response of the different data sets analysed, cf. Figs. 7a and 7b in MSTW08. Entries not given correspond to $\alpha_s(M_Z)$ central values below 0.110 or above 0.130; in case no errors are assigned these are larger than the bounds provided in form of the plots in MSTW08.

$\alpha_s(M_Z^2)$: Correlation with HT

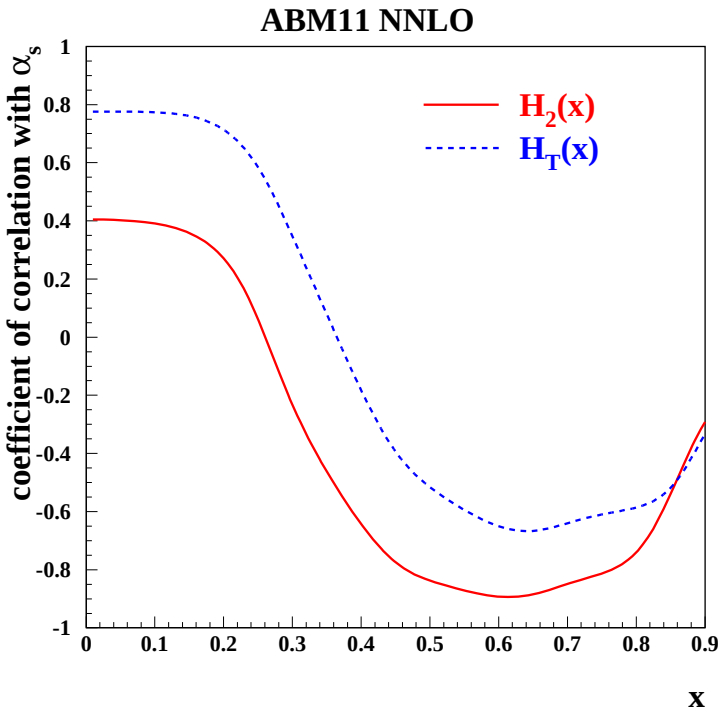

Figure 20: The correlation coefficient of $\alpha_s(M_Z)$ with the nucleon twist-4 coefficients H_2 (solid line) and H_T (dashes) versus x as obtained in our NNLO fit.

$\alpha_s(M_Z^2)$: Global DIS Comparison

Data Set	ABM11	BBG	NN21	MSTW
BCDMS	0.1048 ± 0.0013	0.1126 ± 0.0007	0.1158 ± 0.0015	0.1101 ± 0.0094
NMC	0.1152 ± 0.0007	0.1153 ± 0.0039	0.1150 ± 0.0020	0.1216 ± 0.0074
SLAC	0.1128 ± 0.0003	0.1158 ± 0.0034	> 0.124	$\left\{ \begin{array}{l} 0.1140 \pm 0.0060 \text{ ep} \\ 0.1220 \pm 0.0060 \text{ ed} \end{array} \right.$
HERA	0.1126 ± 0.0002		$\left\{ \begin{array}{l} 0.1199 \pm 0.0019 \\ 0.1231 \pm 0.0030 \end{array} \right.$	0.1208 ± 0.0058
DY	0.101 ± 0.025	–	–	0.1136 ± 0.0100
	0.1134 ± 0.0011	0.1134 ± 0.0020	0.1173 ± 0.0007	0.1171 ± 0.0014

Table 9: Comparison of the pulls in $\alpha_s(M_Z)$ per data set between the ABM11, BBG, NN21, MSTW analyses at NNLO.

Use: $W^2 > 12.5$ GeV^2, $Q^2 > 2.5$ GeV^2 and no HT: $\alpha_s(M_Z^2) = 0.1191 \pm 0.0016$
Use: $W^2 > 12.5$ GeV^2, $Q^2 > 10$ GeV^2 and no HT: $\alpha_s(M_Z^2) = 0.1134 \pm 0.0008$
MSTW08 and NNPDF: no HT corrections.
Taking into account error correlations is of importance.

$\alpha_s(M_Z^2)$: DIS & other NNLO Determinations

	$\alpha_s(M_Z)$	
BBG	$0.1134\ ^{+\ 0.0019}_{-\ 0.0021}$	valence analysis, NNLO
BB	0.1132 ± 0.0022	valence analysis, NNLO
GRS	0.112	valence analysis, NNLO
ABKM	0.1135 ± 0.0014	HQ: FFNS $n_f = 3$
ABKM	0.1129 ± 0.0014	HQ: BSMN-approach
JR	0.1124 ± 0.0020	dynamical approach
JR	0.1158 ± 0.0035	standard fit
ABM11	0.1134 ± 0.0011	
MSTW	0.1171 ± 0.0014	
NN21	0.1173 ± 0.0007	
CT10	0.118 ± 0.005	
Gehrmann et al.	$0.1153 \pm 0.0017 \pm 0.0023$	e^+e^- thrust
Abbate et al.	$0.1135 \pm 0.0011 \pm 0.0006$	e^+e^- thrust
3 jet rate	0.1175 ± 0.0025	Dissertori et al. 2009
Z-decay	0.1189 ± 0.0026	BCK 2008/12 (N^3LO)
τ decay	0.1212 ± 0.0019	BCK 2008
τ decay	0.1204 ± 0.0016	Pich 2011
τ decay	0.1169 ± 0.0025	Boito et al. 2011
lattice	0.1205 ± 0.0010	PACS-CS 2009 (2+1 fl.)
lattice	0.1184 ± 0.0006	HPQCD 2010
lattice	0.1200 ± 0.0014	ETM 2012 (2+1+1 fl.)
lattice	0.1156 ± 0.0022	Brambilla et al. 2012 (2+1 fl.)
BBG	$0.1141\ ^{+\ 0.0020}_{-\ 0.0022}$	valence analysis, $N^3LO(^*)$
BB	0.1137 ± 0.0022	valence analysis, $N^3LO(^*)$
world average	0.1184 ± 0.0007	(2009)
	0.1183 ± 0.0010	(2011)

Table 10: Summary of recent NNLO QCD analyses of the DIS world data, supplemented by related measurements using other processes.

Remark on a recent study on BCDMS

- proposal to reject low y data. $\longrightarrow \Delta\alpha_s(M_Z^2) = +0.0090$ w.r.t. BCDMS
- our analysis: $\alpha_s(M_Z^2) = 0.1139 \pm 0.0012$ NNLO

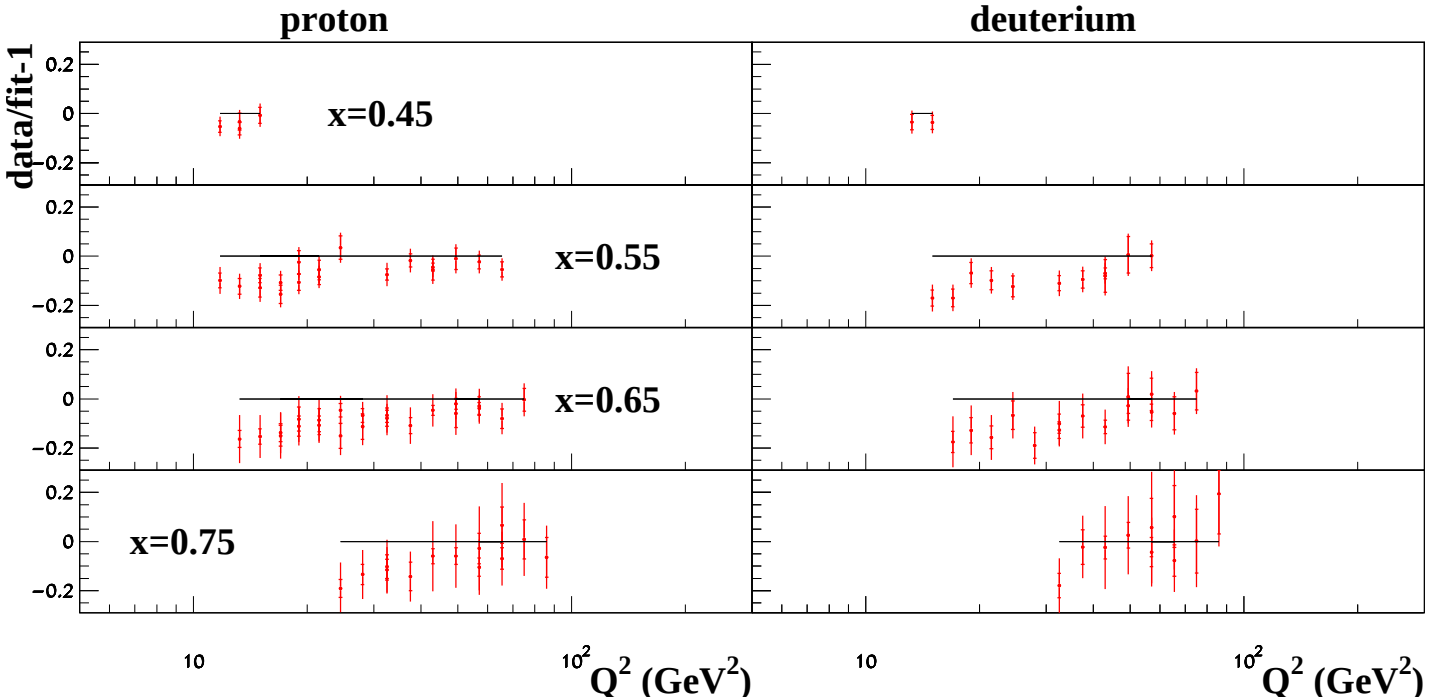

Figure 21: The same as in Fig. 5 for the data points rejected in the analysis of [Shaikhatdenov09].

Heavy Flavor Structure Functions

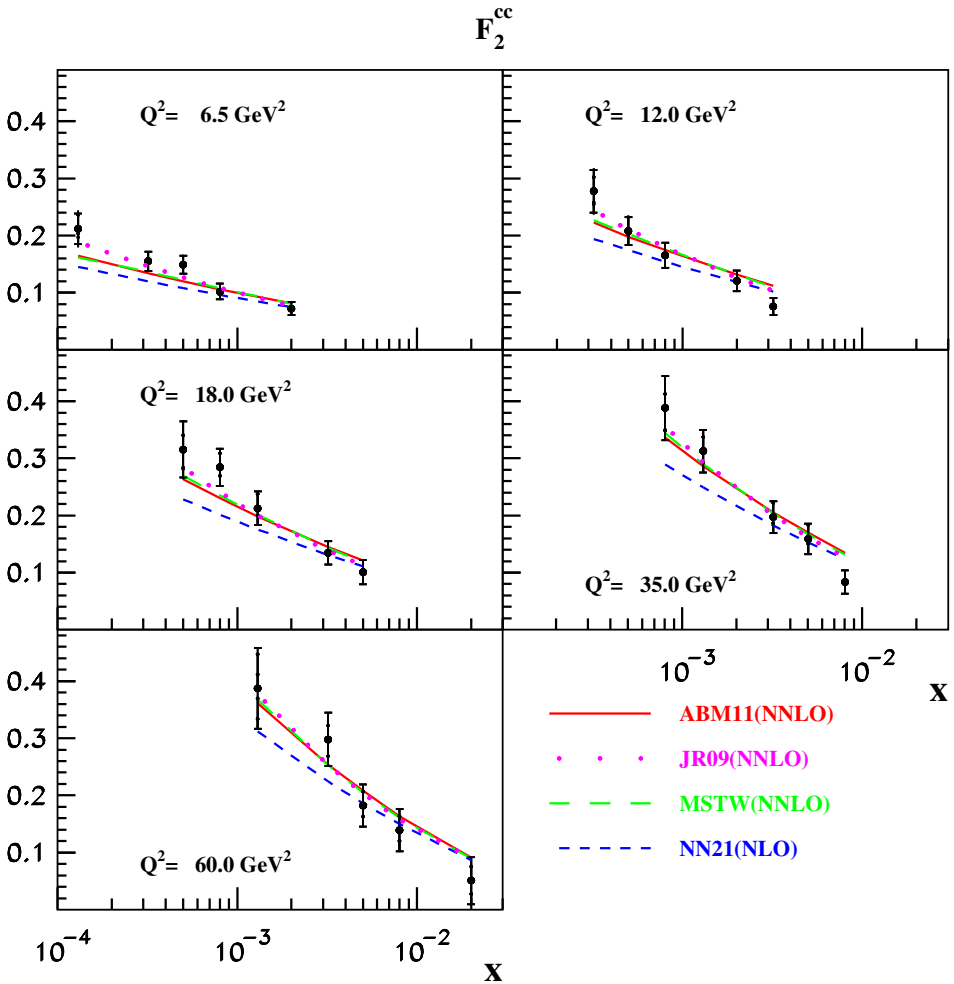

Figure 22: Comparison of the data from [H1-11] for the semi-inclusive structure function F_2^{cc} at different values of the momentum transfer Q^2 versus x with predictions of various PDF sets at NLO and NNLO in QCD, all taken in the FFNS with $n_f = 3$ and with a running-mass of $m_c = 1.27$ GeV The NNLO predictions for F_2^{cc} use the ABM11 PDFs (solid curves), the JR09 PDFs (dots), and the MSTW08 PDFs (long dashes). The NLO calculations are based on the NN21 PDFs (short dashes).

Heavy Flavor Structure Functions

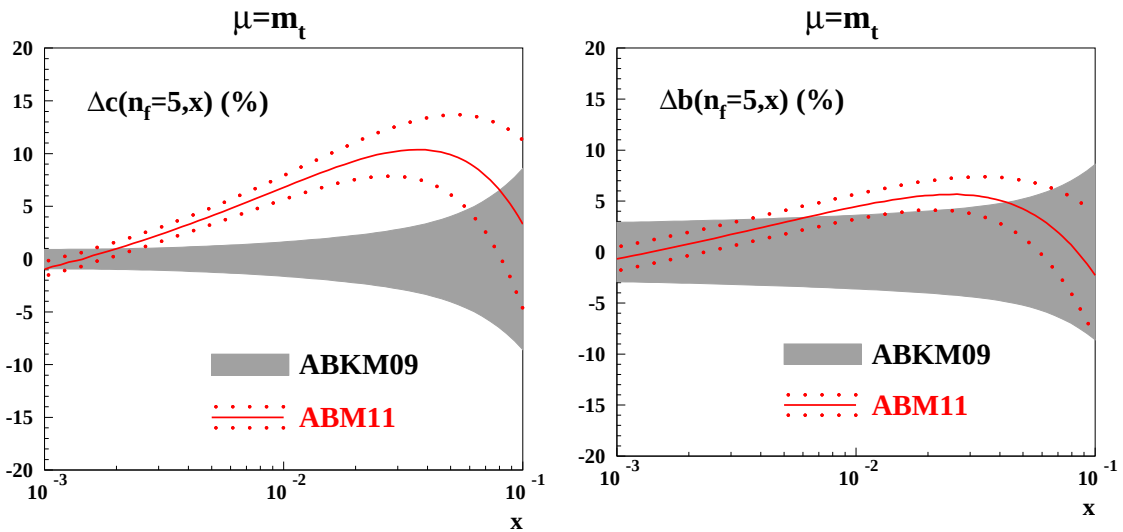

Figure 23: The charm- (left) and the bottom-quark (right) PDFs obtained in the global fit: The dotted (red) lines denote the $\pm 1\sigma$ band of relative uncertainties (in percent) and the solid (red) line indicates the central prediction resulting from the fit with the running masses. For comparison the shaded (grey) area represents the results of ABKM09.

D0 Jet Data

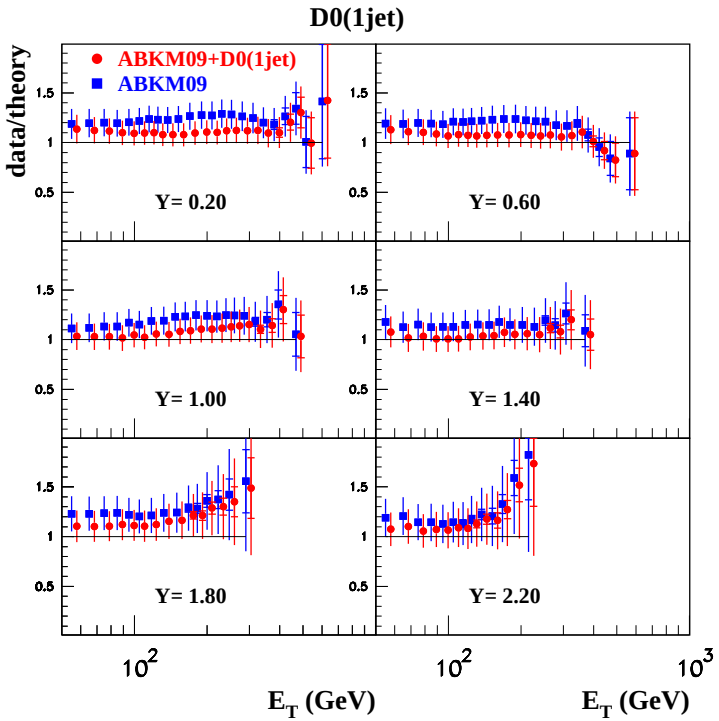

Figure 26: Cross section data for 1-jet inclusive production from the D0 collaboration [Abazov:08] as a function of the jet's transverse energy E_T for the renormalization and factorization scales equal to E_T compared to the result of ABKM09 (circles) and a re-fit including this data (squares) including the NNLO threshold resummation corrections to the jet production [Kidonakis:00].

CDF Jet Data

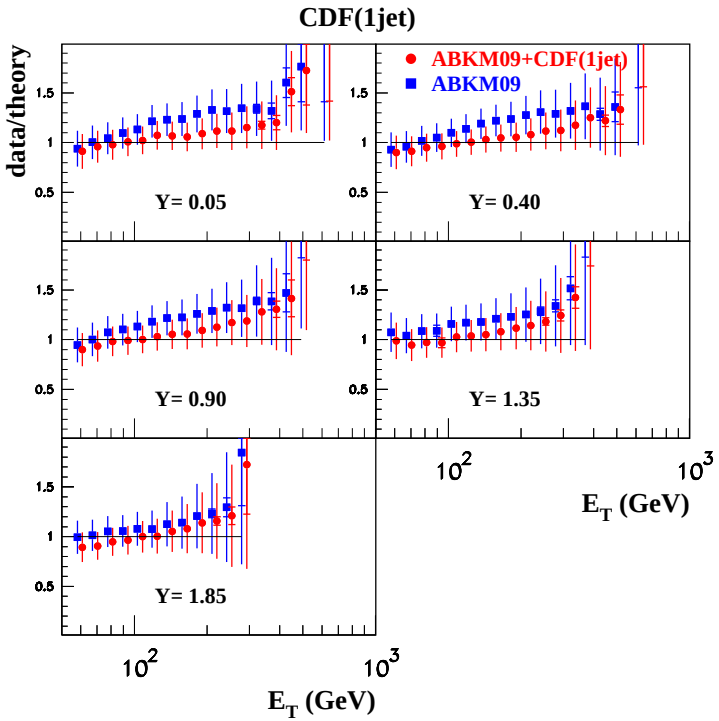

Figure 27: Same as Fig. 26 for the cross section data for 1-jet inclusive production from the CDF collaboration using a k_T jet algorithm [Abulencia:07].

ATLAS Jet Data

NNLO: ABM11: $\alpha_s(M_Z^2) = 0.1134(11)$
ABM11+ATLAS jets: $\alpha_s(M_Z^2) = 0.1141(8)$
NLO: ATLAS: $\alpha_s(M_Z^2) = 0.1151 \pm 0.0047(exp) \pm 0.0023(pdfs)$
Malaescu/Starovoitov '12

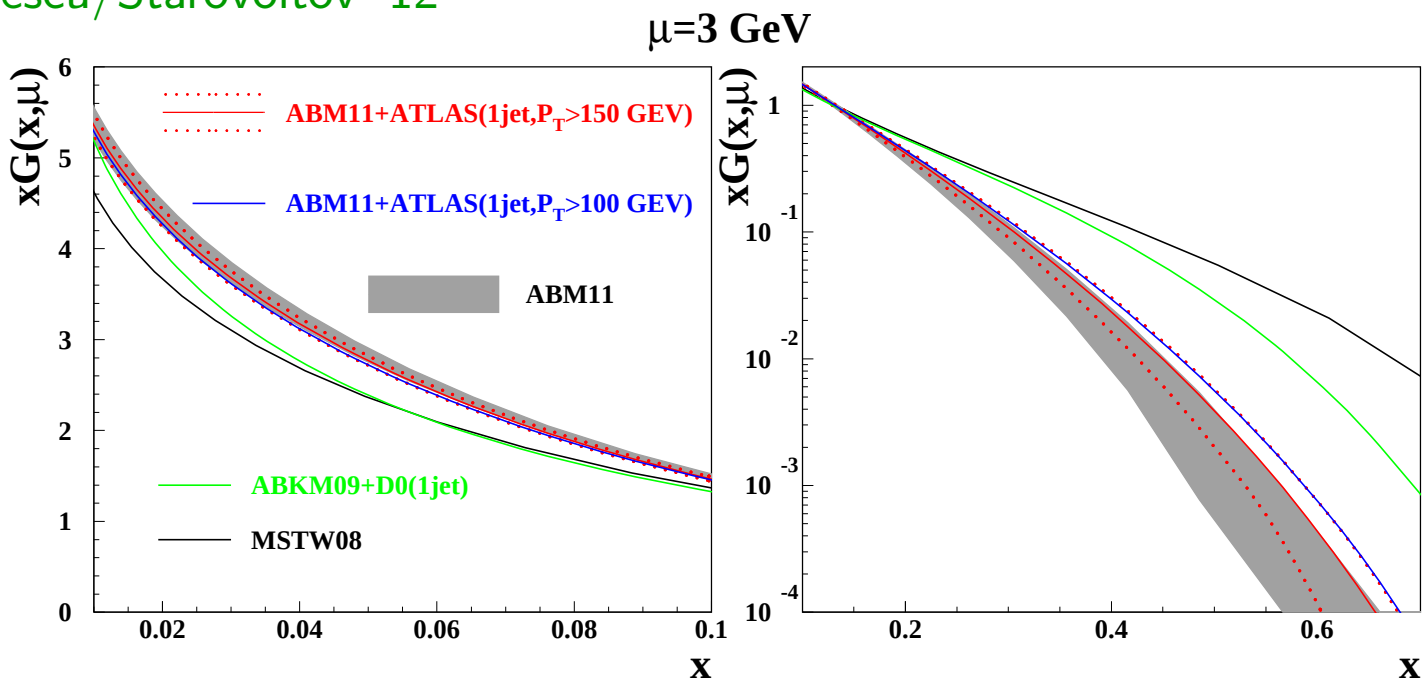

Figure 28: Gluon distribution obtained by including the ATLAS jet data into the ABM11 analysis.

CMS Jets

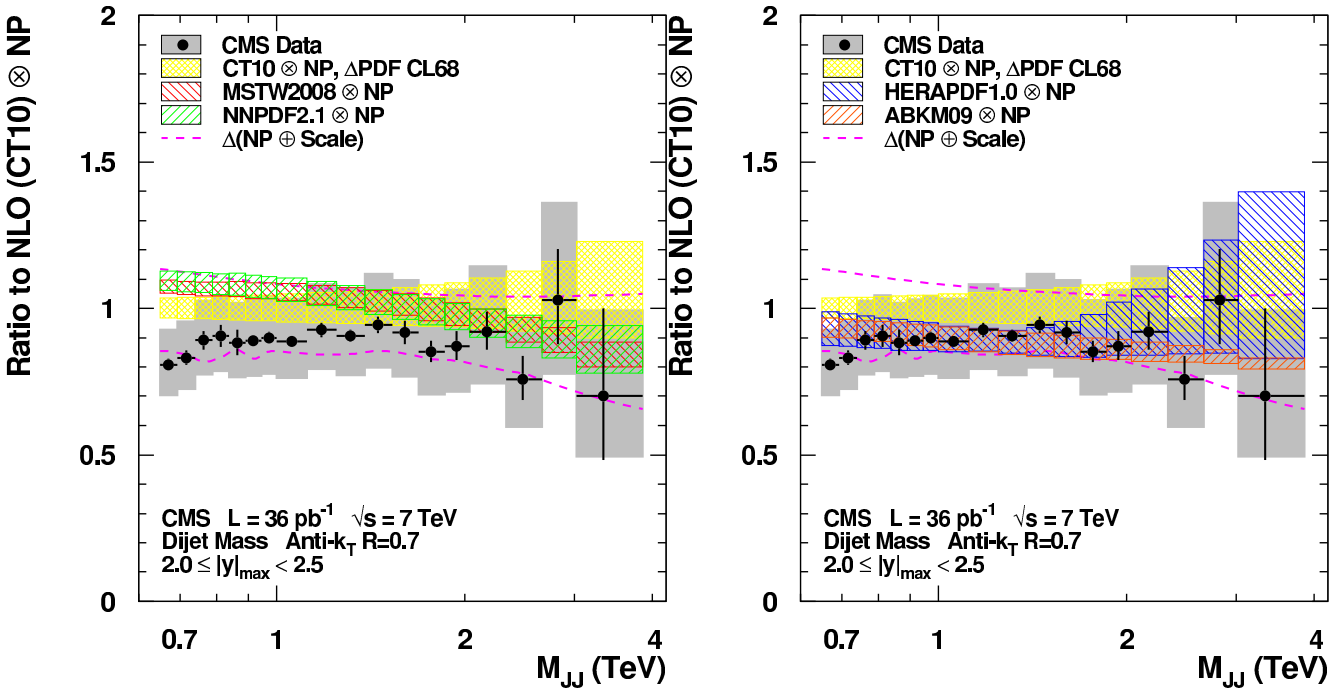

K. Rabbertz et al.: CMS-Note 2011-004.

Charged-lepton Asymmetry

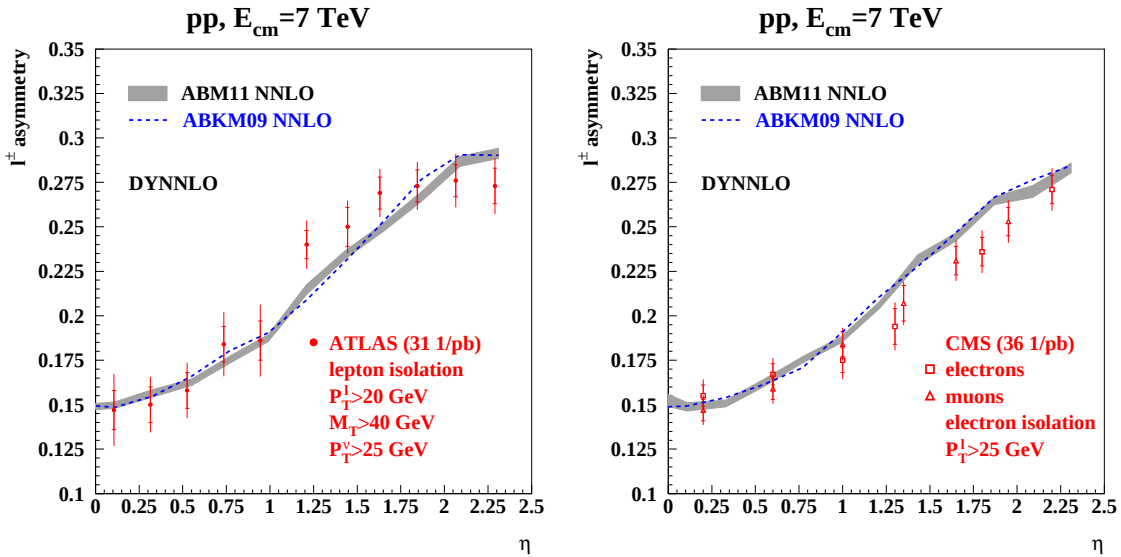

Figure 25: The data on charged-lepton asymmetry versus the lepton pseudo-rapidity η obtained by the ATLAS [Aad:11] (left panel) and CMS [Chatrchyan:11] (right panel) experiments compared to the NNLO predictions based on the `DYNNLO` code [Catani:09/10] and the ABM11 NNLO PDFs with the shaded area showing the integration uncertainties. The ABKM09 NNLO predictions are given for comparison by dashes, without the integration uncertainties shown.

ATLAS & LHCb $W^{\pm}, Z$

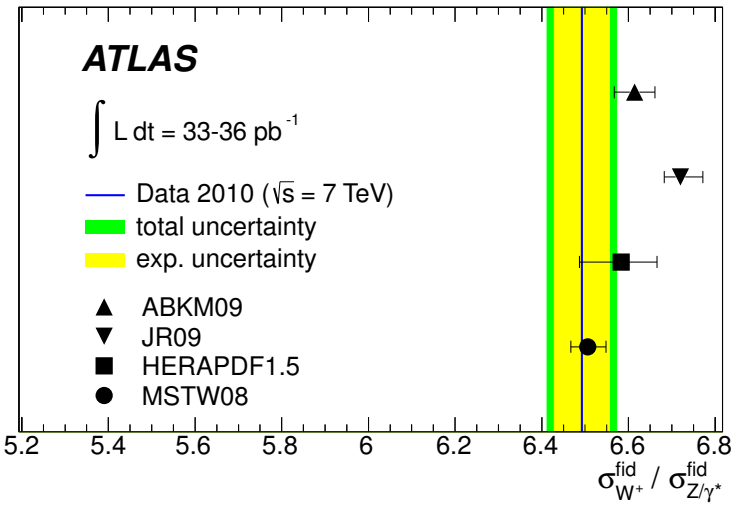

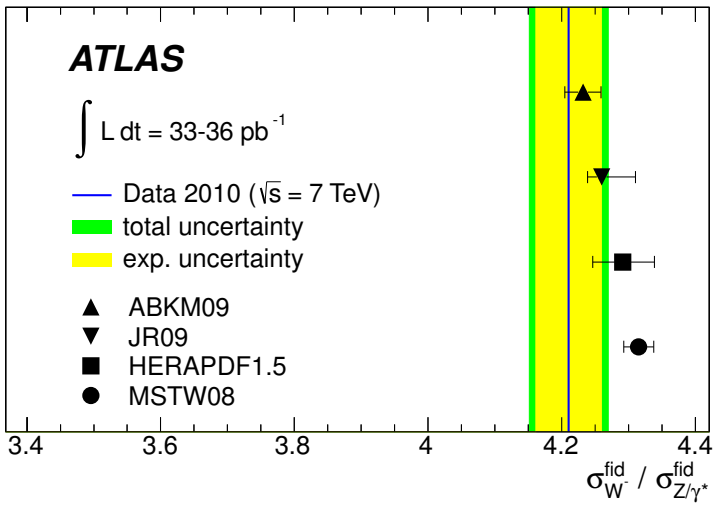

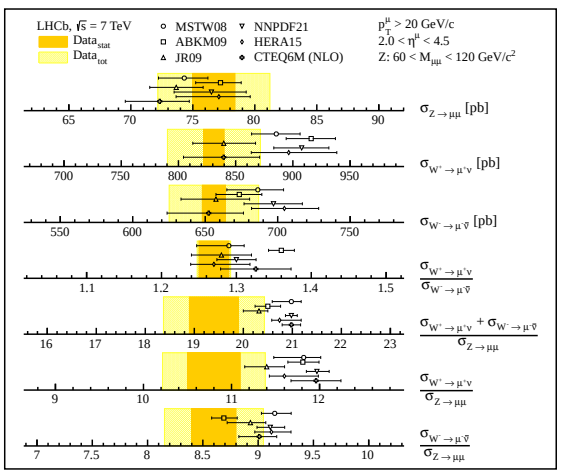

ATLAS: arXiv:1109.5141; LHCb: arXiv:1204.1620

$t\bar{t}$

nb	ABM11	JR09	MSTW	NNPDF21
$\sigma_{t\bar{t}}$ fit m_t	145.5	170.4	175.6	172.7
$\sigma_{t\bar{t}}$ fit $m_t = 160$ GeV	154.4	188.4	192.0	196.9

Calculated with HATHOR: Aliev et al. arXiv:1007.1327

Higgs

$\sigma(pp \to H^0) \propto \alpha_s^2 x G^2(x, Q^2)$.

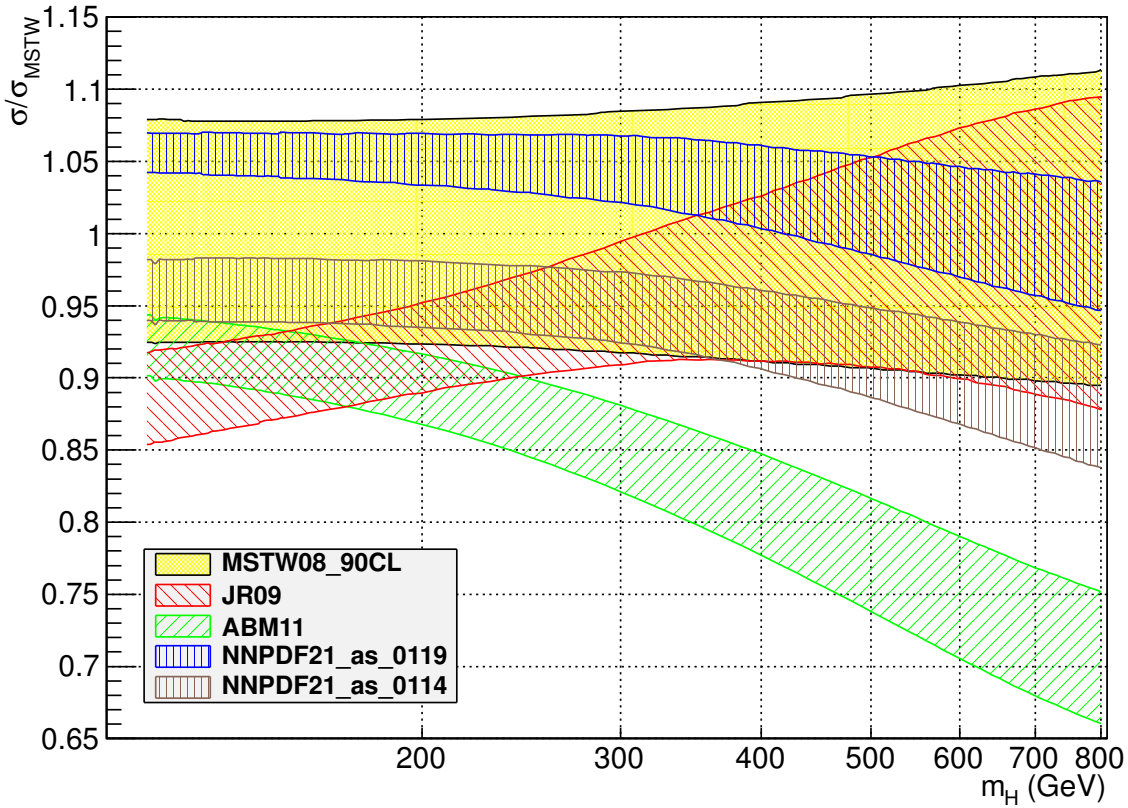

Anastasiou et al., arXiv:1202.3638

DESY

Conclusions

- New ABM11: theory improvements, inclusion of jet data; predicts hadron collider data well
- NNLO: $\alpha_s(M_Z^2) = 0.1134 \pm 0.0011$ vs ABKM09
  $\alpha_s(M_Z^2) = 0.1135 \pm 0.0014$
- The different α_s-values given by MSTW and NNPDF are understood.
- The correct inclusion of systematic error correlations and higher twist effects are important.
- ATLAS jet data analyzed $\rightarrow \alpha_s(M_Z^2) = 0.1141 \pm 0.0008$; the gluon obtained is softer than that in case of Tevatron; Higgs production cross section almost unchanged.
- Inclusive top-cross section: still differences between the groups: $\rightarrow$ $\alpha_s, xg(x, Q^2)$
- LHC data start to constrain sea-quarks $W^{\pm}, Z$, off-resonance Drell-Yan

Conclusions

- LHC data start to constrain the gluon LHC 2,3-jets; these data will improve $\alpha_s(M_Z)$.
- Need of continuous benchmarking
- The "pdf4lhc recommendation" ignored 2 of 3 NNLO analyses since 2009.
  The combined HERA data were not considered in the fits chosen there (but were available).
  All NNLO pdfs are available in LHAPDF and are run very fast.

- Recommendation:
  Use all NNLO pdfs in your final analyses, together with the right value of $\alpha_s(M_Z)$ being correlated, to find out yourself about the remaining systematics.

Comparison to MSTW and NN21: SLAC Data

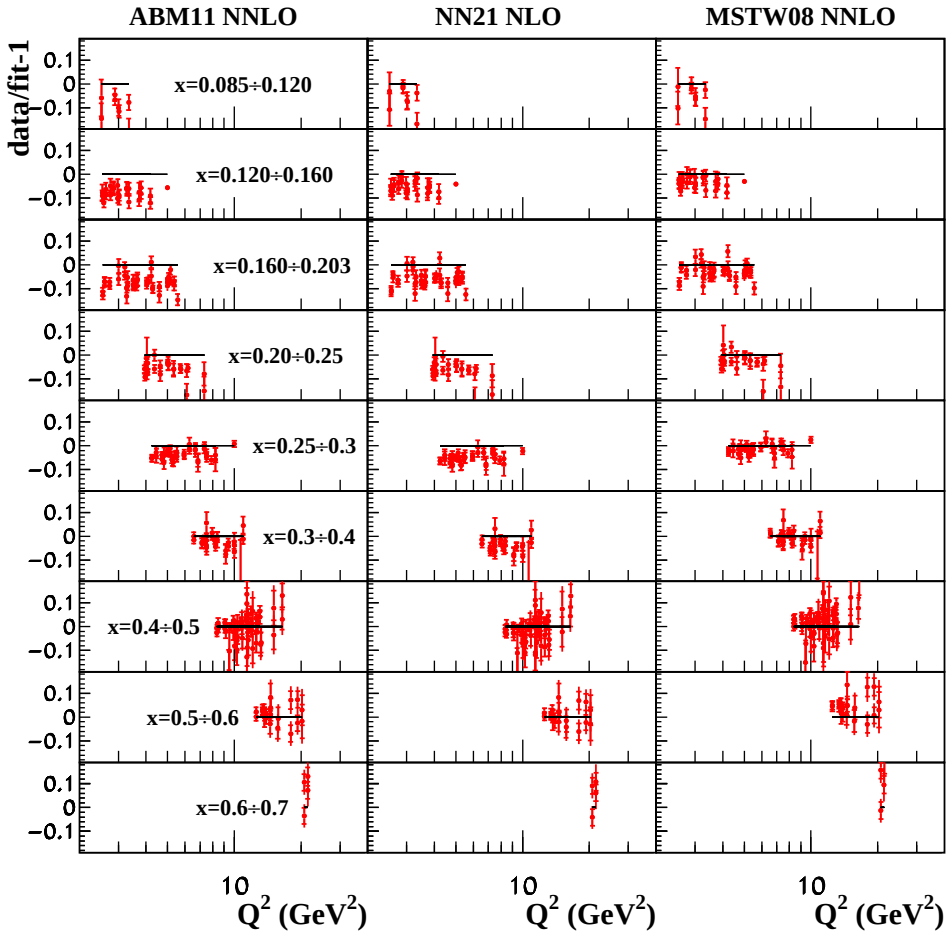

Figure 11: The same as Fig. 7 without the HT terms taken into account and for various 3-flavor PDFs (left panel: present analysis, right panels: MSTW. The NLO calculations based on the 3-flavor NLO NN21 PDFsare given for comparison (central panels). Only the data surviving after the HT-cut are shown; the proton and deuterium data points are superimposed.